

# *BSM Higgs searches with ATLAS*

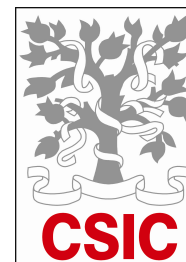
## Higgs Hunting 2016



Luca.Fiorini@cern.ch\*  
(IFIC-U. Valencia-CSIC)  
on behalf of the ATLAS Collaboration

01/09/2016

\*:co-funded by: FPA2015-65652-C4-2-R



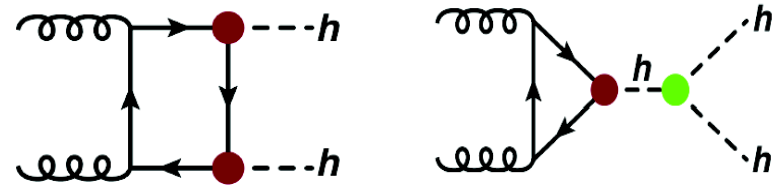
# BSM Higgs Production

- 2 Higgs Doublet Models (2HDM) predict 5 physical bosons:  
 $h, H$  (CP=+1),  $A$  (CP=-1),  $H^+$  and  $H^-$

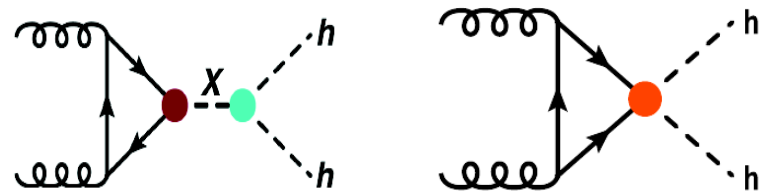
Family	Type-I	Type-II	Lepton-specific	Flipped	Type-III
u	$\Phi_2$	$\Phi_2$	$\Phi_2$	$\Phi_1$	$\Phi_1, \Phi_2$
d	$\Phi_2$	$\Phi_1$	$\Phi_2$	$\Phi_1$	$\Phi_1, \Phi_2$
e	$\Phi_2$	$\Phi_2$	$\Phi_1$	$\Phi_2$	$\Phi_1, \Phi_2$

- MSSM is a special case of type-II 2HDM, often used as benchmark. It can be described by two parameters at tree-level:
  - $\tan\beta = \langle \Phi_2 \rangle / \langle \Phi_1 \rangle$
  - $m_A$ : mass of the CP-odd Higgs boson
- MSSM scenarios commonly used:
  - $m_h^{\max}$  (stop mixing yielding maximum  $m_h$ )
  - $m_h^{\text{mod}\pm}$  (modified stop mixing)
  - **hMSSM**:  $m_h = 125$  GeV used as input to generate the rest of the phenomenology.

- **Di-higgs** production is very small in SM due to destructive interference:
  - 33.7 fb@pp,  $\sqrt{s} = 13$  TeV, non resonant

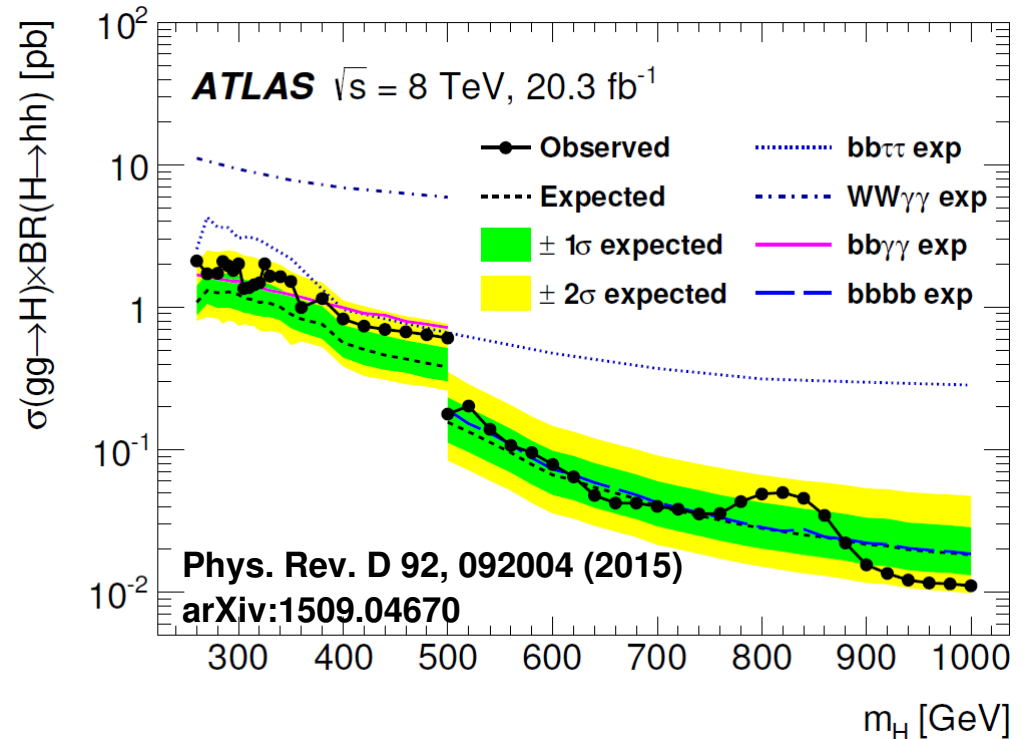
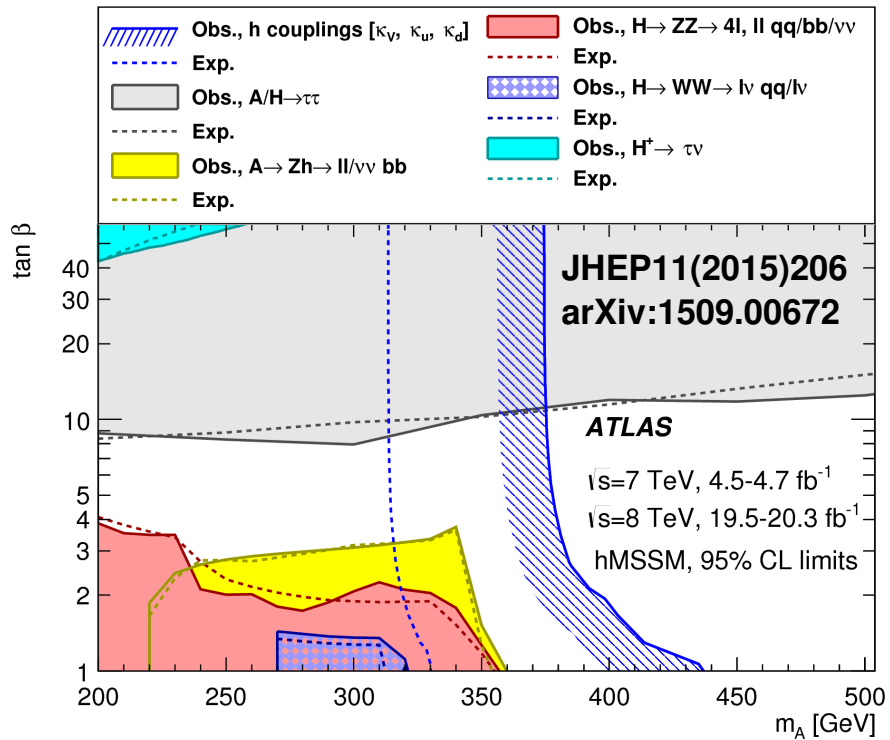


- In BSM, can be enhanced by:
  - Modified top Yukawa coupling or  $\lambda_{hhh}$  (**non-resonant production**).
  - **Resonant** production: 2HDM  $H \rightarrow hh$ , KK gravitons,....



# Run-1 Results Summary

- Panorama at Higgs Hunting 2015
- MSSM: couplings to down-type fermions dominate for high  $\tan\beta$ , couplings to bosons and up-type fermions more important for low  $\tan\beta$ .
- di-Higgs: combined result of  $bbbb$ ,  $bb\gamma\gamma$ ,  $bb\tau\tau$  and  $\gamma\gamma WW$



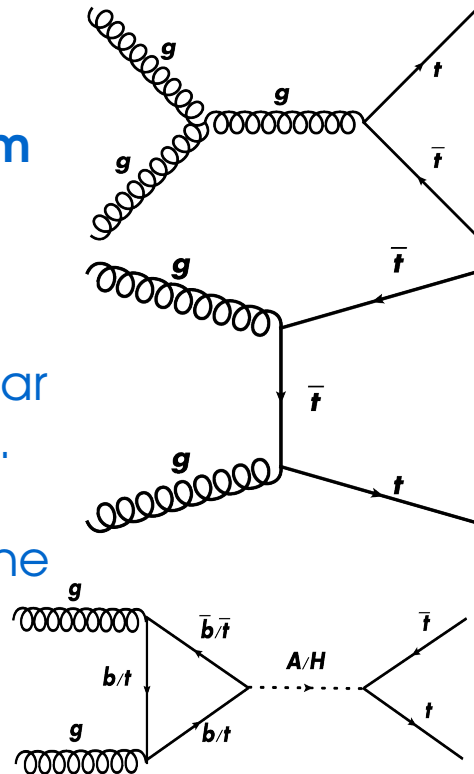
# $H/A \rightarrow \text{Fermions Search}$

## $H/A \rightarrow t\bar{t}$ :

- Branching ratio is larger for low  $\tan\beta$
- Interference between the signal and  $t\bar{t}$  background production modes taken into account.

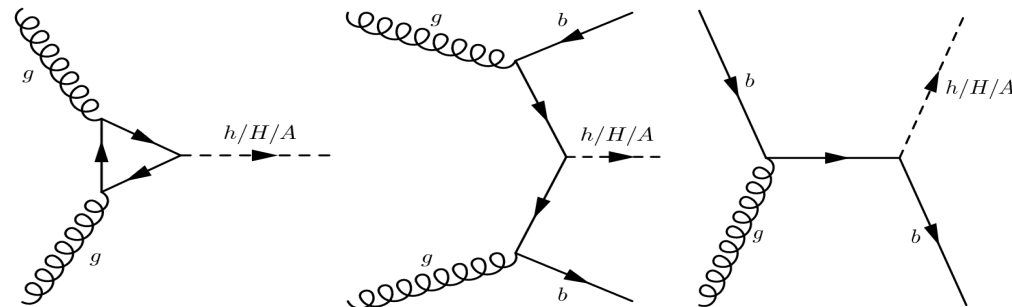
• Signal+Interference obtained from “**diagram subtraction**” and from “**diagram removal**” schemes (Madgraph modified to remove  $t\bar{t}$  background diagrams).

• Difference between the approaches taken as systematics: 0.4%



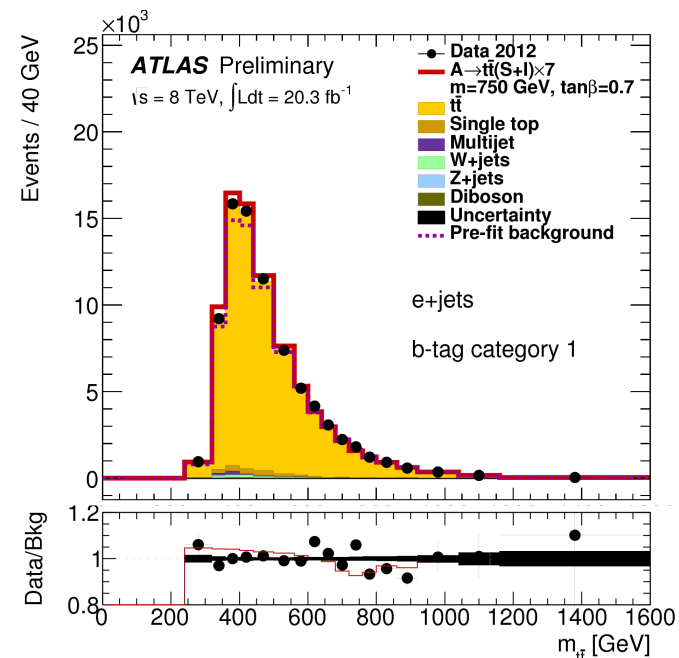
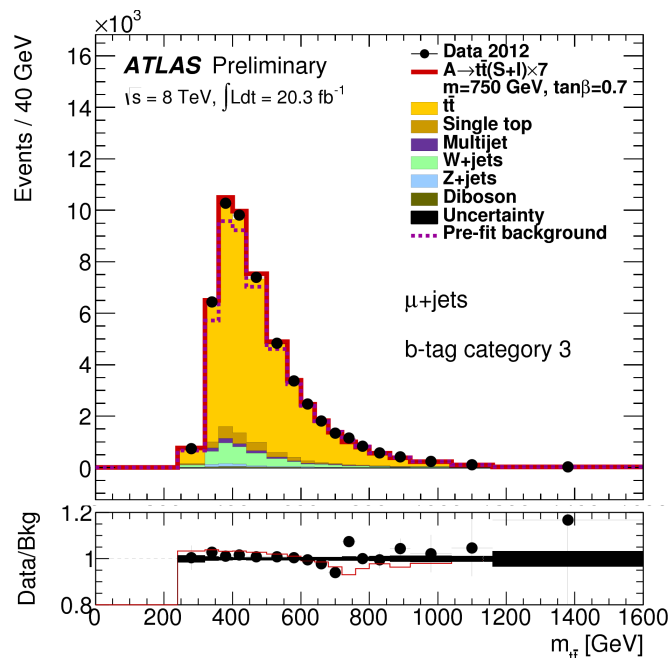
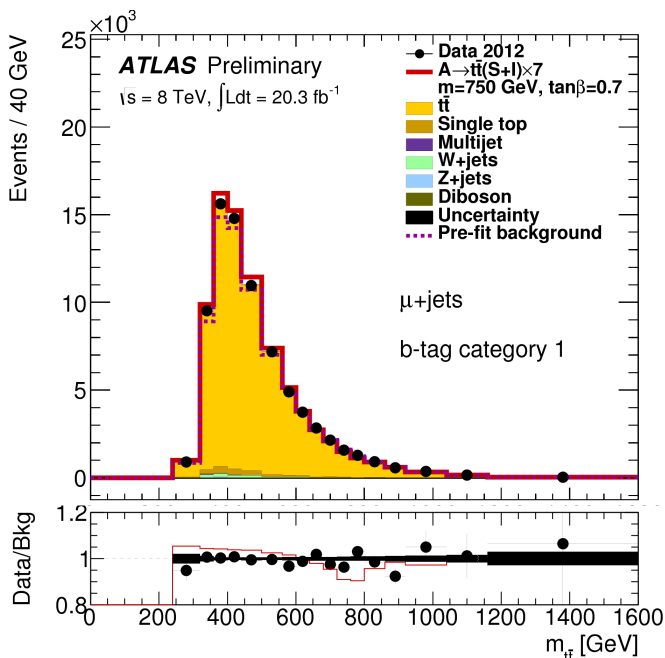
## $H/A \rightarrow \tau\tau$ :

- For  $m_A \gg m_Z$  (decoupling limit) the lightest scalar  $h$  has SM-like couplings;
  - The heavier  $H/A$  bosons are almost degenerate in mass and coupling to  $b$  and  $\tau$  is enhanced for high  $\tan\beta$
- exploit  $b$ -tag and  $b$ -veto categories



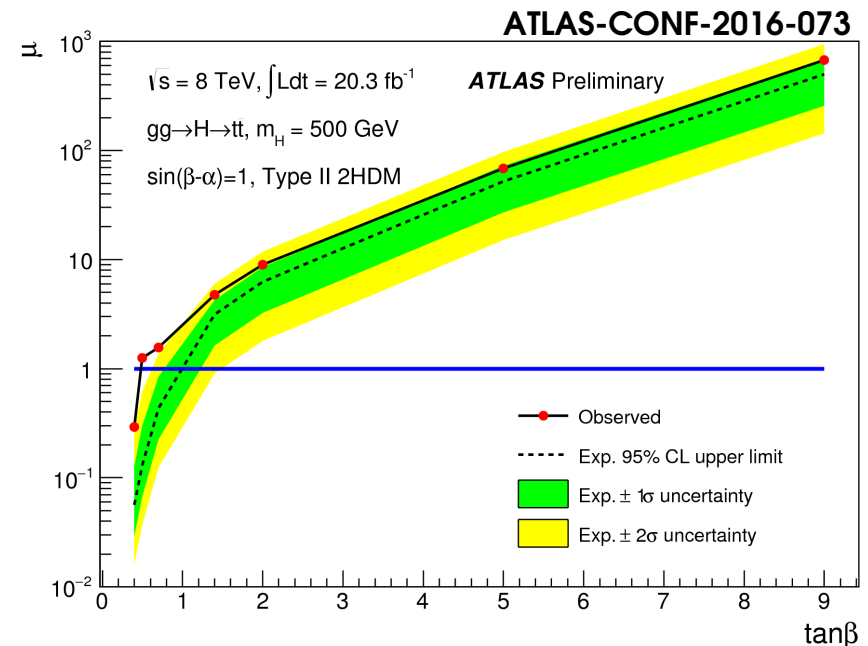
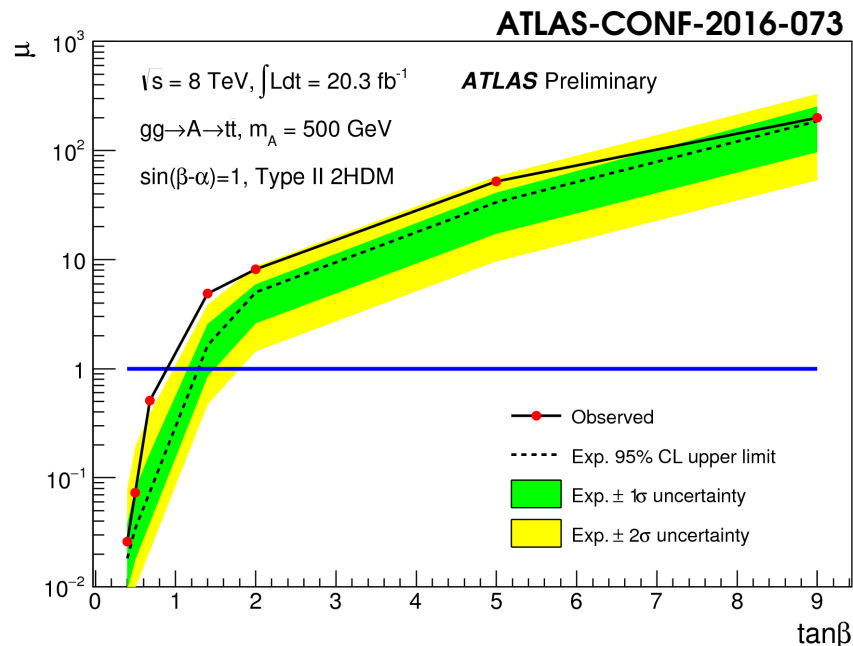
# $H, A \rightarrow t\bar{t}$ Search

- **ATLAS-CONF-2016-073, 20.3 fb<sup>-1</sup> of 8 TeV data**
- Revisit ATLAS Run-1  $t\bar{t}$  resonance search: JHEP 08 (2015) 148
- $e, \mu$  +jets final states, 3  $b$ -tag categories for each final state.
- 4 jets,  $\geq 1$   $b$ -tag jet,  $E_T^{\text{miss}} > 20$  GeV,  $E_T^{\text{miss}} + m_T > 60$  GeV  $m_T^W = \sqrt{2 \cdot p_T^\ell \cdot E_T^{\text{miss}} \cdot (1 - \cos \phi_{\ell\nu})}$
- Kinematic fit ( $\chi^2$ ) of the event (constraints on top and  $W$  masses)
- **Main backgrounds:**  $t\bar{t}$  and  $W$ +jets (the latter estimated from data).



# $H, A \rightarrow t\bar{t}$ Results

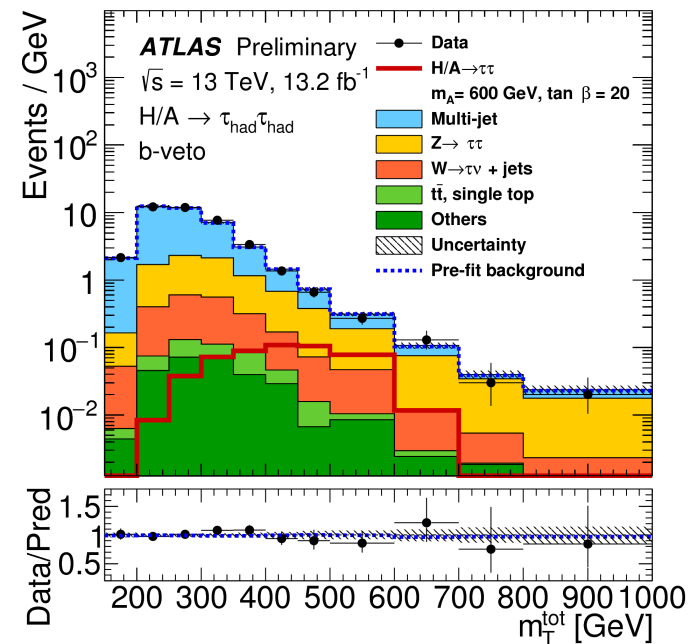
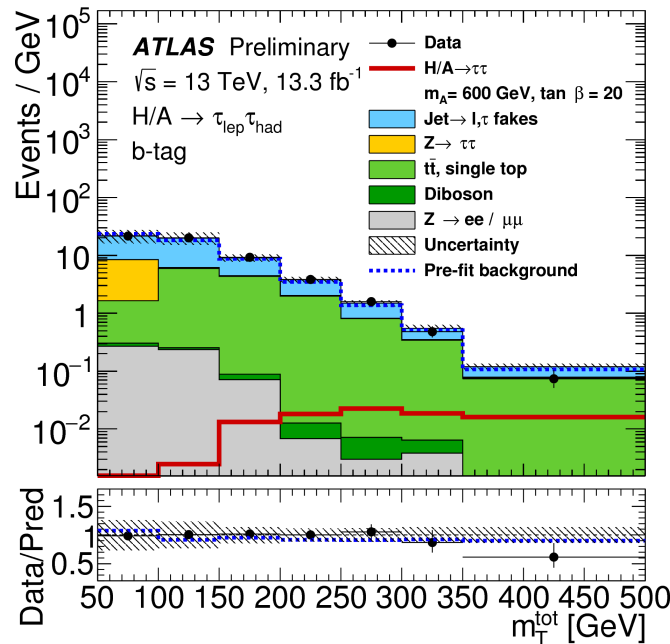
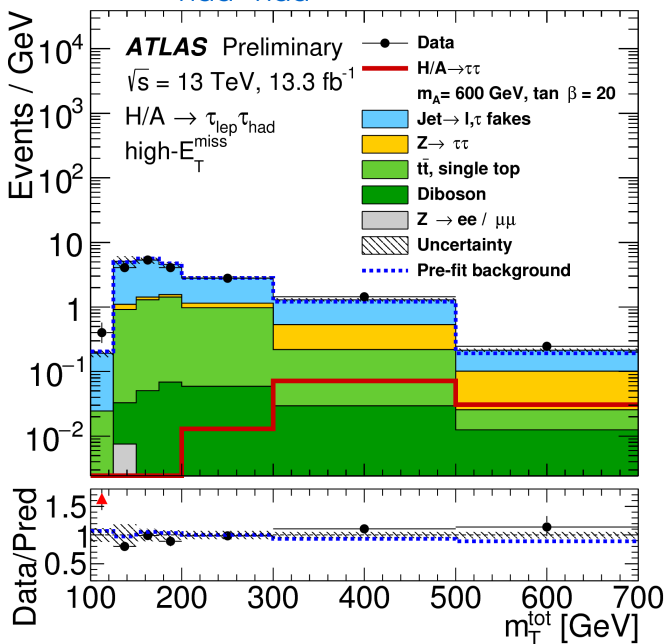
- Upper limits as a function of the parameter  $\tan\beta$  are set for a neutral scalar  $H$  and pseudoscalar  $A$  with benchmark masses of 500 GeV and 750 GeV.
- $\mu=1$  corresponds to the signal strength in a Type-II 2HDM with  $\sin(\beta-\alpha)=1$  and  $m_h = 125$  GeV.



- $\tan\beta < 0.85$  and  $< 0.45$  are excluded for  $m_A=500$  GeV and  $m_H=500$  GeV at 95% CL
- No  $\tan\beta$  values can be excluded for the higher mass point of 750 GeV.

# $H/A \rightarrow \tau\tau$ Search

- **ATLAS-CONF-2016-085,  $\leq 13.3 \text{ fb}^{-1}$  of 13 TeV data**
- $\tau_{\text{lep}}\tau_{\text{had}}$  and  $\tau_{\text{had}}\tau_{\text{had}}$  channels (they dominate the sensitivity at high mass)
- $b$ -tag and  $b$ -veto categories. High- $E_{\text{T}}^{\text{miss}}$  category also used for  $\tau_{\text{lep}}\tau_{\text{had}}$
- $m_{\text{T}}^{\text{tot}}$  variable used in both channels  $m_{\text{T}}^{\text{tot}} = \sqrt{m_{\text{T}}^2(E_{\text{T}}^{\text{miss}}, \tau_1) + m_{\text{T}}^2(E_{\text{T}}^{\text{miss}}, \tau_2) + m_{\text{T}}^2(\tau_1, \tau_2)}$ ,
- **Backgrounds:**
  - $\tau_{\text{lep}}\tau_{\text{had}}$ : multi-jet and W-jets/top estimated with data-driven methods.
  - $\tau_{\text{had}}\tau_{\text{had}}$ : multi-jet and fake taus in other backgrounds: data-driven methods



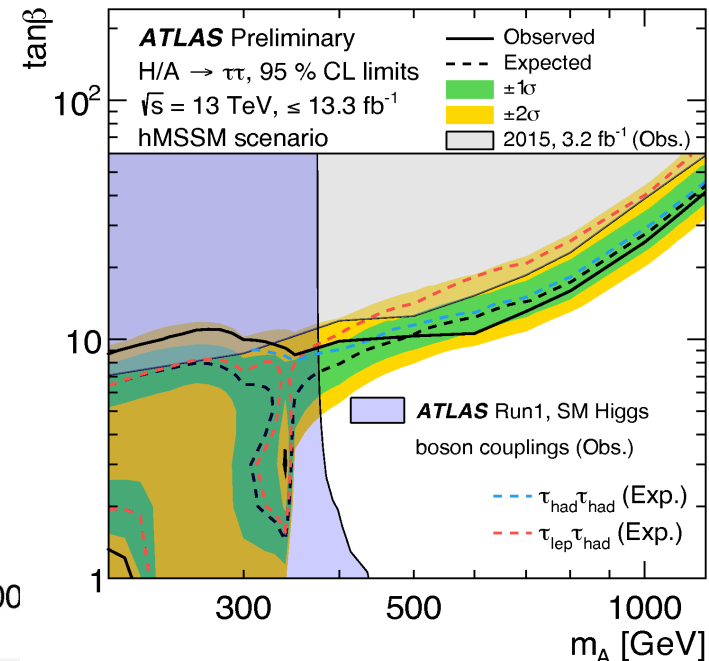
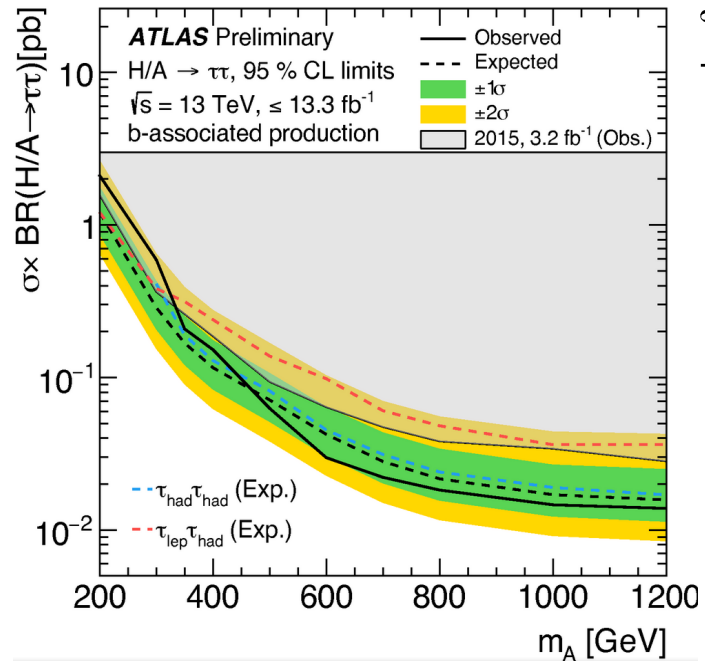
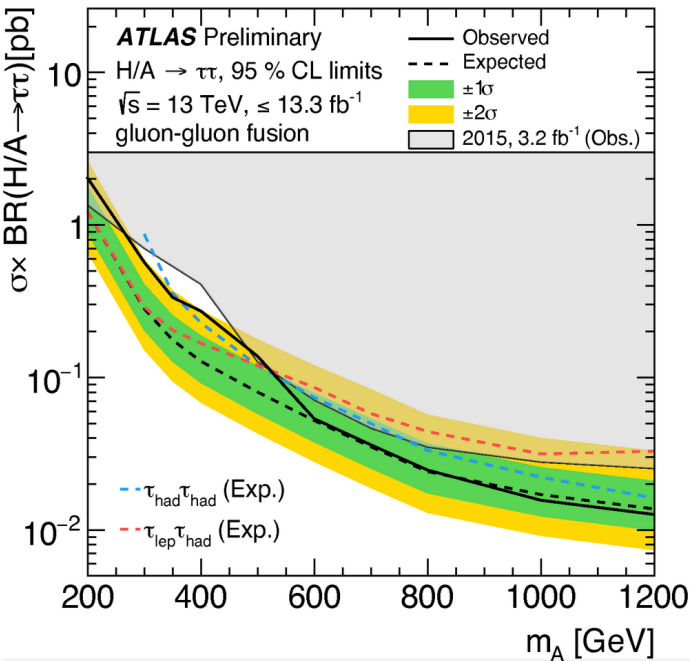
# $H/A \rightarrow \tau\tau$ Results

ATLAS-CONF-2016-085 results: both model independent and MSSM scenarios:

- ggH limits: 2.0-0.013 pb for  $m_A=200-1200$  GeV
- bbH limits: 2.1-0.014 pb for  $m_A=200-1200$  GeV

→ More details in P. De Bruin talk this afternoon!

- Check out also the recently submitted ATLAS paper searching for  $H/A \rightarrow \tau\tau$  and  $Z' \rightarrow \tau\tau$  with  $3.2 \text{ fb}^{-1}$ : [arXiv.org:1608.00890](http://arXiv.org:1608.00890)





# Charged Higgs $H^\pm \rightarrow \tau\nu$ Search

- For  $m_{H^\pm} > m_\tau$ , production in association with top-quark is dominant

- $H^\pm \rightarrow \tau\nu$  search: **ATLAS-CONF-2016-088**

- Discriminant variable is  $m_T$ :

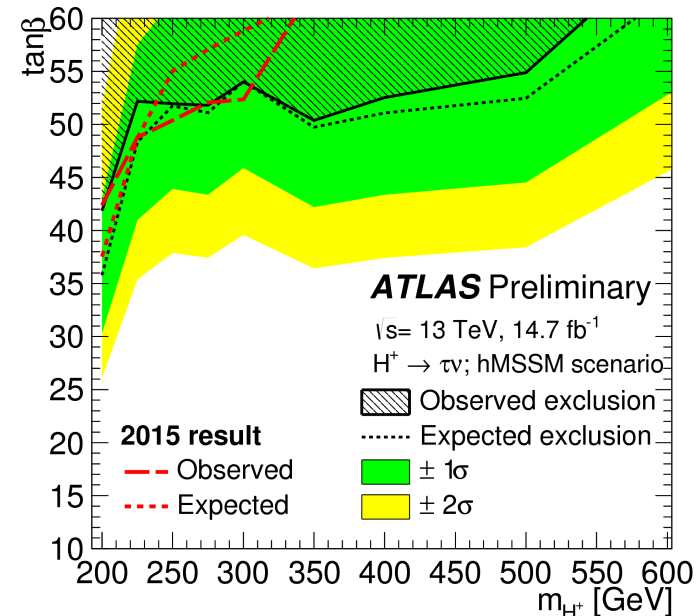
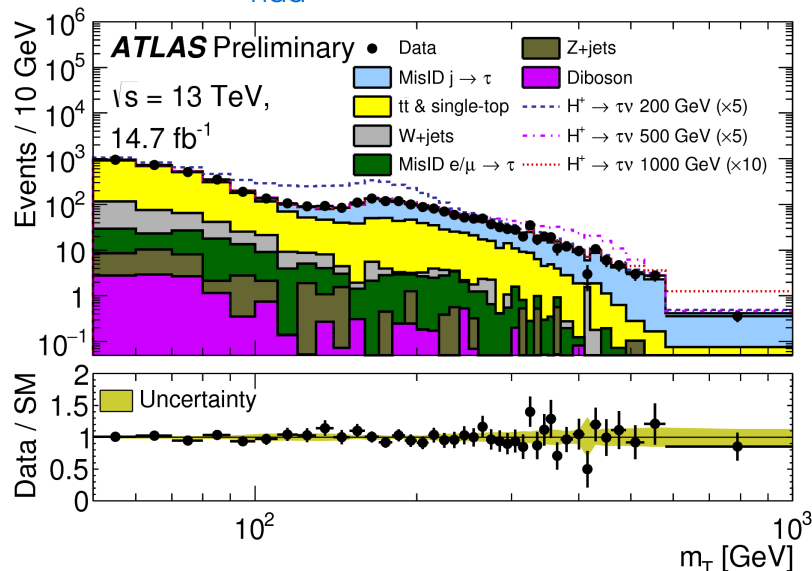
$$m_T = \sqrt{2p_T^\tau E_T^{\text{miss}} (1 - \cos \Delta\phi_{\tau, E_T^{\text{miss}}})}$$

- **Backgrounds:**

- True  $\tau_{\text{had}}$ : MC normalised/checked in CRs with low  $m_T$
- Jet  $\rightarrow \tau_{\text{had}}$  fakes: Fake Factor (FF)

- **Signal Region:**

- 1  $\tau_{\text{had}}$   $p_{T>40}$  GeV
- 3 jets  $p_{T>25}$  GeV ( $\geq 1$   $b$ -tagged jet)
- $E_T^{\text{miss}} > 150$  GeV



Observed hMSSM exclusion:  
 $\tan\beta > 42-60$  @  $m_{H^\pm} = 200-540$  GeV

# Charged Higgs $H^\pm \rightarrow tb$ search

- For  $m_{H^\pm} > m_t$ , production in association with top-quark is dominant

- $H^\pm \rightarrow tb$  search: **ATLAS-CONF-2016-089**

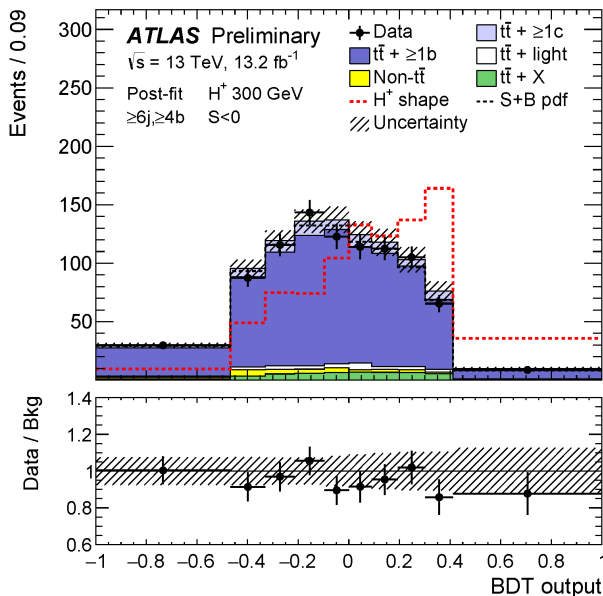
- **lepton+jets final state (lep=e, $\mu$ )**

- Discriminant variable is a BDT-score calculated from 12 input variables

- Signal Regions:

- 1 lepton with  $p_T > 25$  GeV

- $5j3b$ ,  $5j \geq 4b$ ,  $\geq 6j3b$  and  $\geq 6j \geq 4b$

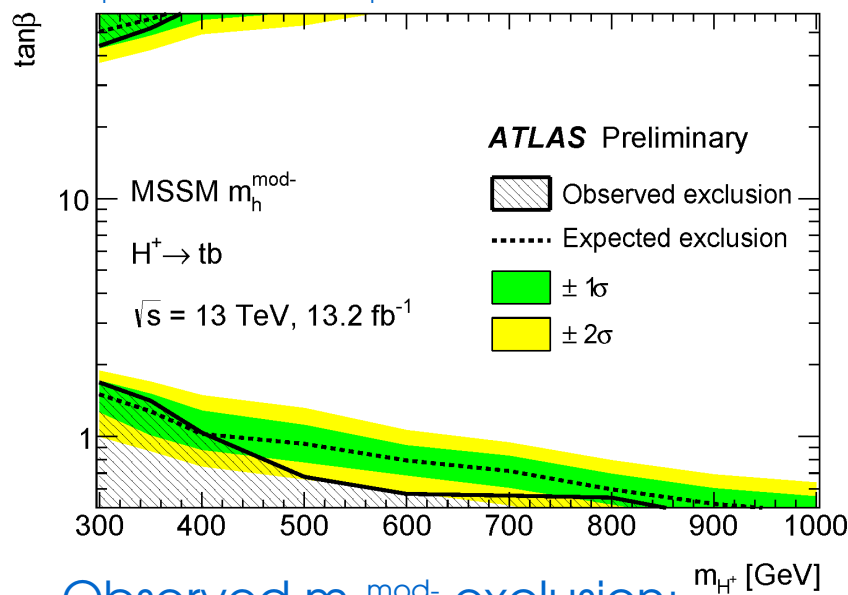


- **Backgrounds:**

- $t\bar{t}$ bar+jets production dominates, modelled using Powheg + Pythia6: reweight  $t\bar{t}$ bar+light and  $t\bar{t}$ bar+ $\geq 1c$  to NNLO and  $t\bar{t}$ bar+ $\geq 1b$  to NLO

- Control Regions:  $4j2b$ ,  $4j \geq 3b$ ,  $5j2b$  and  $\geq 6j2b$

- $H_T^{\text{had}}$  (Sum of  $p_T$  of selected jets) used for CR

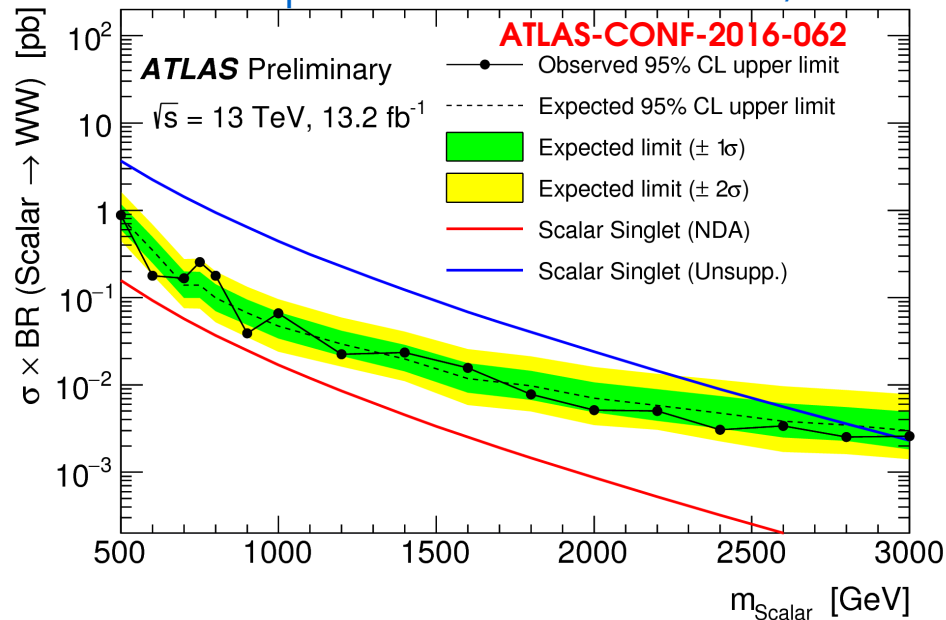


Observed  $m_h^{\text{mod-}}$  exclusion:

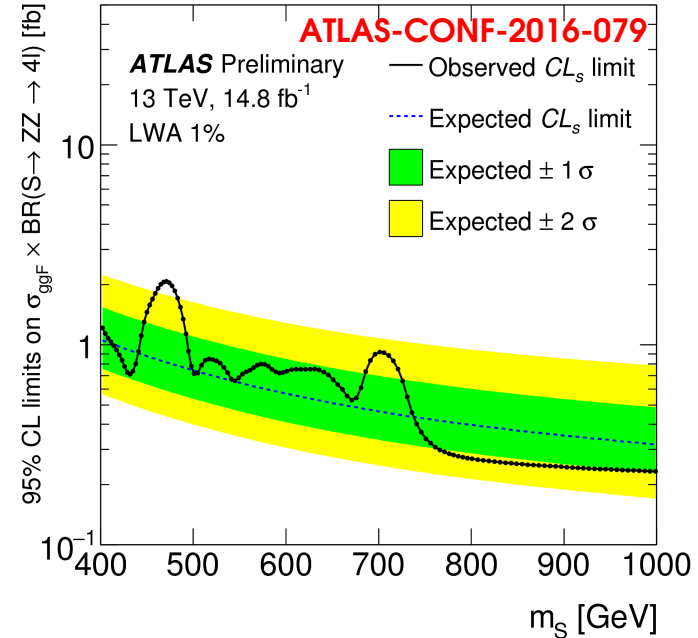
$\tan\beta < 1.7-0.5$  @  $m_{H^\pm} = 300-855$  GeV

# $H \rightarrow WW \rightarrow lvqq$ and $H \rightarrow ZZ \rightarrow 4l$ searches

- $H \rightarrow WW \rightarrow lvqq'$  ( $l=e,\mu$ ):  $13.2 \text{ fb}^{-1}$  @ 13 TeV
- **Selection:**  $e,\mu + E_T^{\text{miss}} > 100 \text{ GeV}$ ,  $\geq 1$  R=1 jet
- Likelihood fit with dedicated control regions for  $t\bar{t}$  and  $W$ +jets
- Signal Regions:
  - High/Low-purity: pass/fail  $D_2^{\beta=1}$  selection
  - $D_{2,\beta=1}$  jet substructure variable for boostV vs QCD separation: [arXiv:1409.6298](https://arxiv.org/abs/1409.6298), [1507.03018](https://arxiv.org/abs/1507.03018)



- $H \rightarrow ZZ \rightarrow 4l$  ( $l=e,\mu$ ):  $14.8 \text{ fb}^{-1}$  @ 13 TeV
- Same selection as SM, but requires both Z on-shell
- **VBF-enriched category:**  $m_{jj} > 400 \text{ GeV}$  and  $\Delta\eta_{jj} > 3.3$
- **ggH-enriched category:** the rest
- Limits set for VBF and ggH production and 4.07 MeV, 1%, 5% and 10% widths



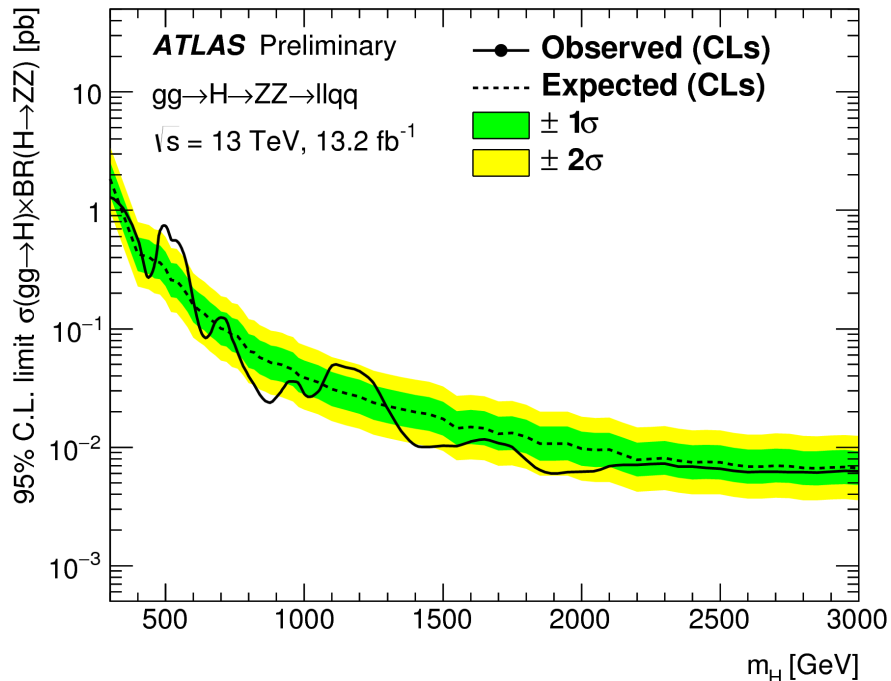
# $H \rightarrow ZZ \rightarrow llqq$ and $\nu\nu qq$ Searches

• **ATLAS-CONF-2016-082,  $13.2 \text{ fb}^{-1}$  @  $13 \text{ TeV}$**

• Searches for a heavy H and a  $W'$  of heavy vector triplet (HVT) model

**$H \rightarrow ZZ \rightarrow llqq$  and  $W' \rightarrow ZW \rightarrow llqq$  searches:**

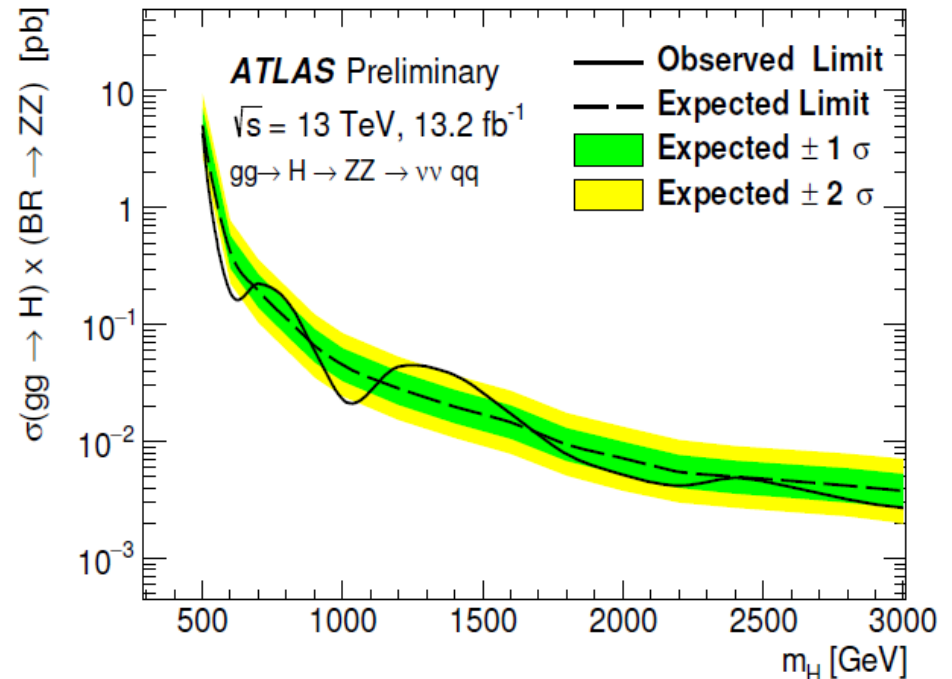
- merged and resolved (2  $b$ -tag and rest) jets final states.
- VBF- and ggF-enriched categories
- Discriminant variables are  $m(\text{ll}J)$  and  $m(\text{ll}jj)$



**$H \rightarrow ZZ \rightarrow \nu\nu qq$  and  $W' \rightarrow ZW \rightarrow \nu\nu qq$  searches:**

- $E_T^{\text{miss}} > 250 \text{ GeV}$  and  $\geq 1$   $R=1$  jet
- Two categories (pass/fail  $D_2^{\beta=1}$  selection)
- Discriminant variable is  $m_T(\nu\nu J)$ :

$$m_T = \sqrt{(E_{T,J} + E_T^{\text{miss}})^2 - (\vec{p}_{T,J} + \vec{E}_T^{\text{miss}})^2}$$



# $hh \rightarrow bbbb$ Search

- **ATLAS-CONF-2016-049**, 13.3 fb<sup>-1</sup> of 13 TeV data.
- **Resolved search**: optimized for low mass and non-resonant regimes
  - 4  $b$ -tagged jets ( $R=0.4$ ), jet pairing using  $\Delta R_{jj}$  and  $m_h$  constraints.
- **Boosted search**: optimized for high mass resonances, where the two  $b$ -jets of the Higgs boson decay cannot be resolved.
  - 2  $R=1$  jets, each of them containing at least 1  $R=0.2$  track jet
  - Events split in 2,3,4 tag categories, based on the number of track jets.
- **Main backgrounds**: multi-jet and  $t\bar{t}$  for both searches
- **Resolved Analysis**:
  - multi-jet: data-driven
  - $t\bar{t}$ : modelled with MC
- **Boosted Analysis**:
  - multi-jet: data-driven
  - $t\bar{t}$ : data-driven normalization, shape from MC
- **Systematic Uncertainties**:
  - $b$ -tagging is the main systematic uncertainty for both analyses.

# $hh \rightarrow bbbb$ Results, ATLAS-CONF-2016-049

- **Results:**
- 95% CL limit is ( $pp \rightarrow hh \rightarrow bbbb$ )  $< 330$  fb

## Resolved

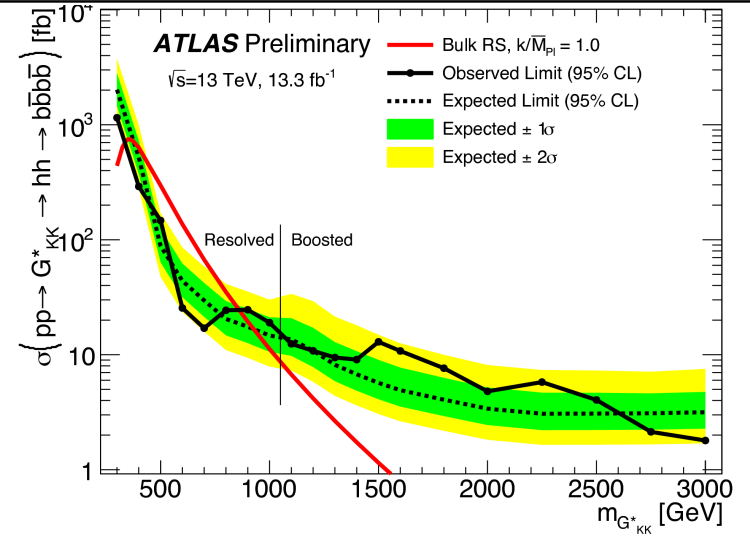
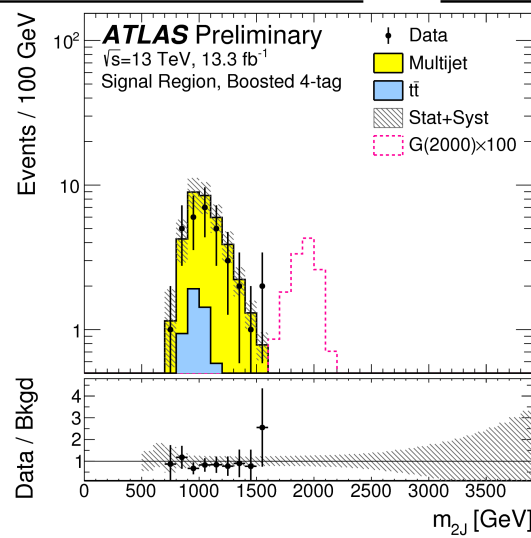
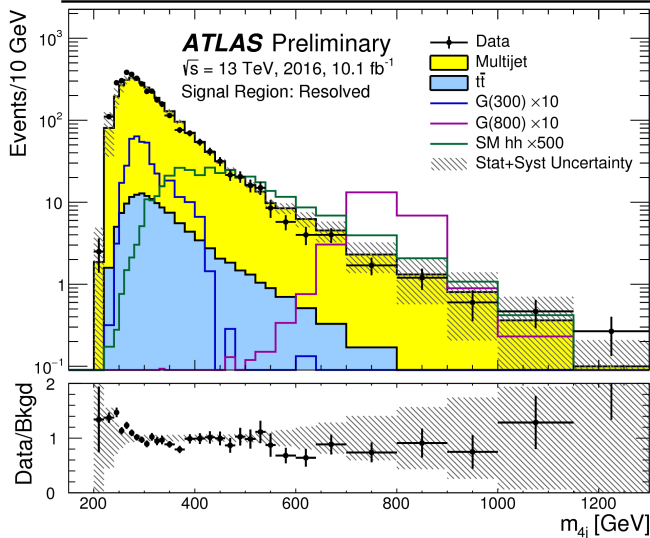
Sample	2015 Signal Region	2016 Signal Region
Multijet	$1\,131 \pm 68$	$3\,670 \pm 200$
$t\bar{t}$	$57 \pm 34$	$190 \pm 110$
Total	$1\,189 \pm 76$	$3\,860 \pm 230$
Data	1 231	3 990
SM $hh$	$0.47 \pm 0.12$	$1.5 \pm 0.4$
$G_{KK}^*$ (800 GeV), $k/\bar{M}_{PI} = 1$	$8 \pm 3$	$24 \pm 8$

- **Excluded mass range:**

- **observed:**  $360 \text{ GeV} < m(G_{KK}^*) < 860 \text{ GeV}$   
(expected:  $380 \text{ GeV} < m(G_{KK}^*) < 910 \text{ GeV}$ )

## Boosted

Sample	2-tag-split	3-tag	4-tag
Multijet	$2\,310 \pm 240$	$515 \pm 41$	$32.6 \pm 7.6$
$t\bar{t}$	$460 \pm 170$	$81 \pm 37$	$5.7 \pm 5.2$
Total	$2\,770 \pm 130$	$596 \pm 39$	$38.3 \pm 9.0$
Data	2 813	671	32
$G_{KK}^*$ (2 TeV), $k/\bar{M}_{PI} = 1$	$0.17 \pm 0.10$	$0.31 \pm 0.06$	$0.15 \pm 0.06$



Check also [arXiv:1606.04782](https://arxiv.org/abs/1606.04782) with  $L=3.2 \text{ fb}^{-1}$  for  $H \rightarrow hh$  specific interpretation.

# Summary

- Several new searches with 13 TeV have been recently released for charged and neutral Higgs bosons, investigating both fermionic and bosonic final states.
  - Impressive performance of the LHC machine during the last months allowed to significantly improve limits on  $\sigma \times \text{BR}$  set over wider mass-ranges and final states, but no significant excess was observed.
  - We are still at the beginning of Run-2 in terms of delivered luminosity, exciting times ahead of us!
- 
- **Additional 13 TeV results with  $>13 \text{ fb}^{-1}$  data recently released by ATLAS**, apologies if your favorite search was not shown in this talk!
- 
- |  |                     |                                      |  |
|--|---------------------|--------------------------------------|--|
| • $H \rightarrow WW \rightarrow l\nu l\nu$ :                     | ATLAS-CONF-2016-074 | → <u>shown by P. Rados yesterday</u> |  |
| • $H \rightarrow ZZ \rightarrow ll\nu\nu$ :                      | ATLAS-CONF-2016-056 |                                      | • $X \rightarrow Z/W\text{h} \rightarrow qqbb$ : ATLAS-CONF-2016-083 |
| • $X \rightarrow H(\gamma\gamma) + E_{\text{T}}^{\text{miss}}$ : | ATLAS-CONF-2016-087 |                                      | • $X \rightarrow VV$ : ATLAS-CONF-2016-055                           |
| • $hh \rightarrow WW\gamma\gamma$ :                              | ATLAS-CONF-2016-071 |                                      | • $H^{\pm\pm} \rightarrow e^{\pm}e^{\pm}$ : ATLAS-CONF-2016-051      |

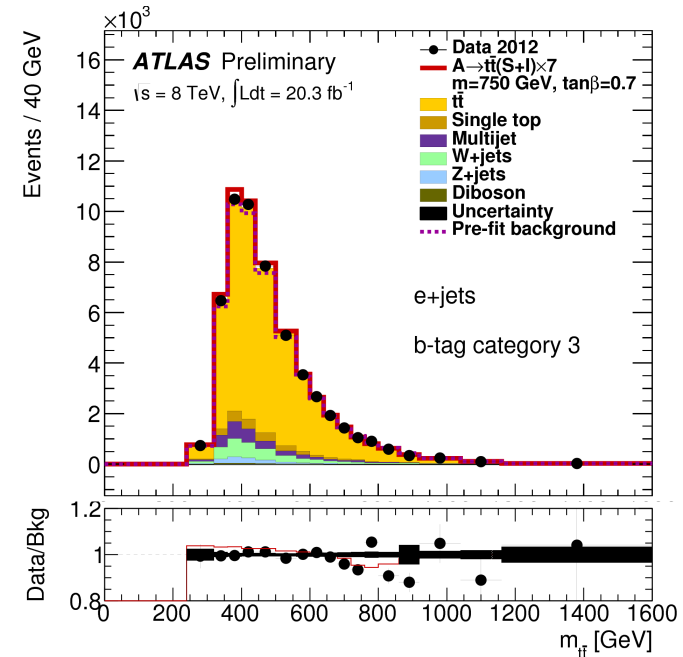
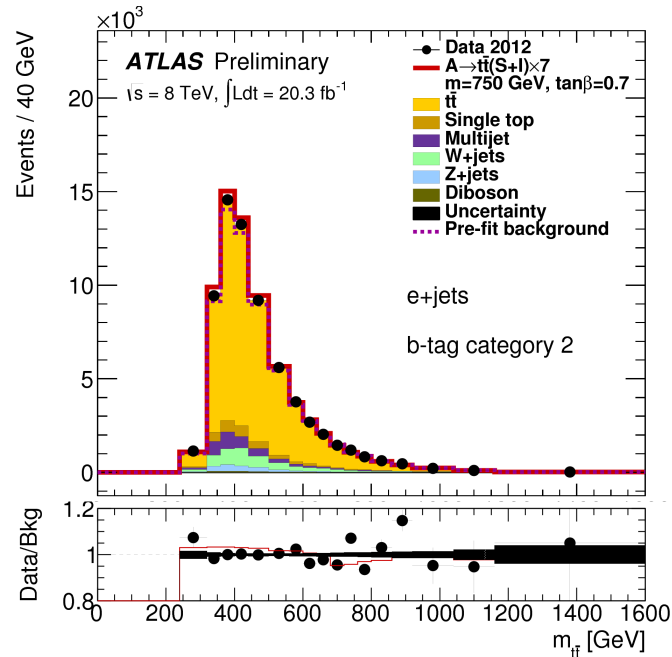
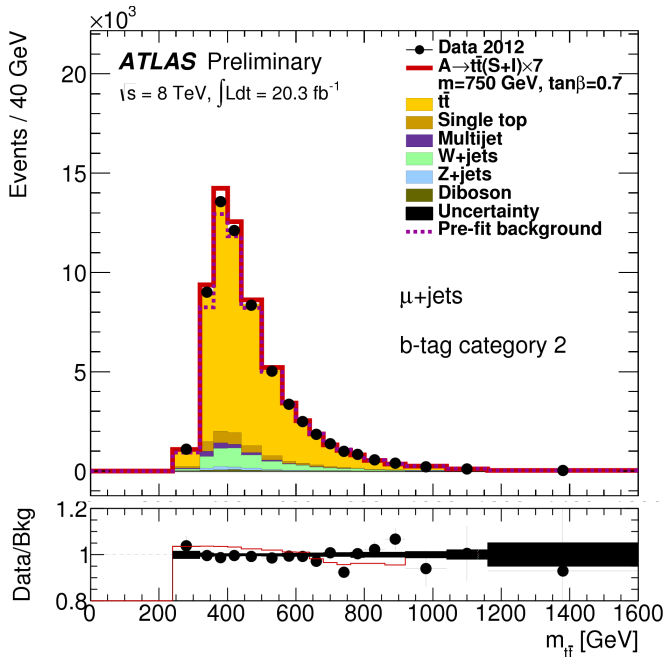
<https://twiki.cern.ch/twiki/bin/view/AtlasPublic/HiggsPublicResults>

*Backup*



# $H, A \rightarrow t\bar{t}$ Search

- **ATLAS-CONF-2016-073, 20.3 fb<sup>-1</sup> of 8 TeV data**
- $b$ -tag categories:
  - category 1:  $b$ -tagged jet assigned to each of the hadronically and semileptonically decaying top-quark candidates by the  $\chi^2$  algorithm.
  - category 2:  $b$ -tagged jet assigned only to the hadronically
  - category 3:  $b$ -tagged jet assigned only to the semileptonically decaying top quark



# $H, A \rightarrow t\bar{t}b\bar{a}r$ Search (2)

- Main systematics are:
  - jet energy scale (JES), 4% (1%) for central jets with a transverse momentum of 20 GeV (1 TeV)
  - jet reconstruction efficiency
  - jet energy resolution (JER).
  - The combined impact of the JES and JER uncertainties on the event yields is 6% for the total background, 4% for the pure resonant signal  $S$  of a pseudoscalar resonance with a mass of  $m_A = 500$  GeV and  $\tan \beta = 0.68$ , and 8% for the corresponding  $S+I$  component.

Type	$e$ +jets	$\mu$ +jets	Sum
$t\bar{t}$	95,000 $\pm$ 11,000	93,000 $\pm$ 11,000	188,000 $\pm$ 22,000
Single top quark	3,900 $\pm$ 500	3,800 $\pm$ 500	7,700 $\pm$ 1,000
$t\bar{t}V$	290 $\pm$ 40	280 $\pm$ 40	560 $\pm$ 80
$W$ +jets	6,600 $\pm$ 2,100	7,200 $\pm$ 2,300	13,800 $\pm$ 4,300
$Z$ +jets	1,400 $\pm$ 620	650 $\pm$ 250	2,100 $\pm$ 900
Diboson	320 $\pm$ 120	310 $\pm$ 120	630 $\pm$ 240
Multijet $e$	5,300 $\pm$ 1,100	-	5,300 $\pm$ 1,100
Multijet $\mu$	-	1,060 $\pm$ 230	1,060 $\pm$ 30
Total	112,000 $\pm$ 13,000	106,000 $\pm$ 12,000	219,000 $\pm$ 25,000
Data	115,785	110,218	226,003

Table 2: Data and expected background event yields after the resolved-topology selection. The uncertainty on the expected background yields is derived by summing all systematic uncertainties and the MC statistical uncertainty in quadrature. The expected yields and uncertainties are shown before the profile likelihood fit (described in the text) to the full dataset.

# $H/A \rightarrow \tau\tau$ Signal and Control Regions

$\tau_{\text{lep}}\tau_{\text{had}}$ signal region	$\Delta\phi(\tau_{\text{had-vis}}, \ell) > 2.4$ , $m_{\text{T}}(\ell, E_{\text{T}}^{\text{miss}}) < 40 \text{ GeV}$ , Veto $80 < m_{e,\tau} < 110 \text{ GeV}$ for $\tau_e\tau_{\text{had}}$ ,
high- $E_{\text{T}}^{\text{miss}}$ category:	$E_{\text{T}}^{\text{miss}} ( \vec{p}_{\text{T}}(\mu) + \vec{E}_{\text{T}}^{\text{miss}} ) > 150 \text{ GeV}$ for $\tau_e\tau_{\text{had}}$ ( $\tau_{\mu}\tau_{\text{had}}$ ),
$b$ -tag/ $b$ -veto categories:	fail high- $E_{\text{T}}^{\text{miss}}$ category requirements, $N_{b\text{-tag}} \geq 1$ ( $b$ -tag category), $N_{b\text{-tag}} = 0$ ( $b$ -veto category)
$b$ -veto/ $t\bar{t}$ fake-factor control region	$m_{\text{T}}(\ell, E_{\text{T}}^{\text{miss}}) > 70$ (60) $\text{GeV}$ for $\tau_e\tau_{\text{had}}$ ( $\tau_{\mu}\tau_{\text{had}}$ ), $N_{b\text{-tag}} = 0$ different $\tau_{\text{had-vis}}$ identification for the anti- $\tau_{\text{had}}$ region
$b$ -tag control region	$N_{b\text{-tag}} \geq 1$ , $m_{\text{T}}(\ell, E_{\text{T}}^{\text{miss}}) > 100 \text{ GeV}$
Multi-jet fake-factor control region	invert $e, \mu$ isolation requirement, $N_{b\text{-tag}} \geq 1$ ( $b$ -tag category), $N_{b\text{-tag}} = 0$ ( $b$ -veto and high- $E_{\text{T}}^{\text{miss}}$ categories) different $\tau_{\text{had-vis}}$ identification for the anti- $\tau_{\text{had}}$ multi-jet control region
Multi-jet control region for $\tau_{\text{MJ}}$ estimation	$m_{\text{T}}(\ell, E_{\text{T}}^{\text{miss}}) < 30 \text{ GeV}$ , no $e, \mu$ isolation requirement, no $\tau_{\text{had-vis}}$ passing loose identification, $N_{\text{jet}} \geq 1$ and $N_{b\text{-tag}} = 0$ ( $b$ -veto category), $N_{\text{jet}} \geq 2$ and $N_{b\text{-tag}} \geq 1$ ( $b$ -tag category), $N_{\text{jet}} \geq 1$ , $N_{b\text{-tag}} = 0$ and $E_{\text{T}}^{\text{miss}} ( \vec{p}_{\text{T}}(\mu) + \vec{E}_{\text{T}}^{\text{miss}} ) > 150 \text{ GeV}$ for $\tau_e\tau_{\text{had}}$ ( $\tau_{\mu}\tau_{\text{had}}$ ) (high- $E_{\text{T}}^{\text{miss}}$ category)
$\tau_{\text{had}}\tau_{\text{had}}$ signal region	$\Delta\phi(\tau_{\text{had-vis},1}, \tau_{\text{had-vis},2}) > 2.7$ , $N_{b\text{-tag}} \geq 1$ and $p_{\text{T}} > 65 \text{ GeV}$ for the sub-leading $\tau_{\text{had-vis}}$ ( $b$ -tag category), $N_{b\text{-tag}} = 0$ ( $b$ -veto category)
Multi-jet fake-factor control region	pass single-jet trigger, leading $\tau_{\text{had-vis}}$ with $p_{\text{T}} > 100 \text{ GeV}$ that fails medium identification, no charge requirements and for leading $\tau_{\text{had-vis}}$ $n_{\text{tracks}} \leq 7$ ( $b$ -tag category), $n_{\text{tracks}} = 1, 3$ ( $b$ -veto category), $\frac{p_{\text{T}}^{\tau_{\text{had-vis},2}}}{p_{\text{T}}^{\tau_{\text{had-vis},1}}} > 0.3$
Fake rate control region	pass single-muon trigger, isolated muon with $p_{\text{T}} > 55 \text{ GeV}$ , $\tau_{\text{had-vis}}$ with $p_{\text{T}} > 50 \text{ GeV}$ , $\Delta\phi(\mu, \tau_{\text{had-vis}}) > 2.4$ , $m_{\text{T}}(\mu, E_{\text{T}}^{\text{miss}}) > 40 \text{ GeV}$ % $\sum_{L=\mu,\tau} \cos \Delta\phi(L, E_{\text{T}}^{\text{miss}}) < 0$ (for $b$ -veto category only) $N_{b\text{-tag}} \geq 1$ ( $b$ -tag category), $N_{b\text{-tag}} = 0$ ( $b$ -veto category)
Same-sign validation region	The two $\tau_{\text{had-vis}}$ objects are required to have the same electric charge

# $H/A \rightarrow \tau\tau$ Systematics

Source of uncertainty	$F_-$ (%)	$F_+$ (%)
$t\bar{t}$ background parton shower model	-21	+39
$\tau_{\text{had-vis}}$ energy scale, detector modelling	-10	+12
$r_{\text{MJ}}$ estimation $b$ -veto region ( $\tau_\mu\tau_{\text{had}}$ )	- 5	+ 6
$r_{\text{MJ}}$ estimation $b$ -veto region ( $\tau_e\tau_{\text{had}}$ )	- 2.3	+ 3.0
$bbH$ signal cross-section uncertainty	- 3.8	+ 1.6
Multi-jet background ( $\tau_{\text{had}}\tau_{\text{had}}$ )	- 2.2	+ 2.6
Jet-to- $\tau_{\text{had-vis}}$ fake rate $b$ -veto region ( $\tau_{\text{lep}}\tau_{\text{had}}$ )	- 1.3	+ 2.9
$\tau_{\text{had-vis}}$ energy scale, in-situ calibration	- 1.4	+ 1.1
$r_{\text{MJ}}$ estimation high- $E_{\text{T}}^{\text{miss}}$ region ( $\tau_\mu\tau_{\text{had}}$ )	- 1.4	+ 1.0
$\tau$ trigger (2016)	- 0.5	+ 1.3
Statistics (data and simulation)	-48	+25

# $H^\pm \rightarrow \tau\nu$ Systematics

Sample	Event yield
True $\tau_{\text{had}}$	
$t\bar{t}$ & single-top-quark	2880 $\pm$ 770 $\pm$ 25
$W \rightarrow \tau\nu$	265 $\pm$ 51 $\pm$ 18
$Z \rightarrow \tau\tau$	43 $\pm$ 6.8 $\pm$ 7.6
diboson ( $WW, WZ, ZZ$ )	13.8 $\pm$ 2.2 $\pm$ 1.7
Misidentified $e, \mu \rightarrow \tau_{\text{had-vis}}$	126 $\pm$ 24 $\pm$ 6.5
Misidentified jet $\rightarrow \tau_{\text{had-vis}}$	1170 $\pm$ 110 $\pm$ 16
All backgrounds	4500 $\pm$ 800 $\pm$ 36
$H^+$ (200 GeV), hMSSM $\tan\beta = 60$	523 $\pm$ 86 $\pm$ 4
$H^+$ (1000 GeV), hMSSM $\tan\beta = 60$	7.5 $\pm$ 0.6 $\pm$ 0.05
Data	4645

Table 1: Expected event yields for the backgrounds and a hypothetical  $H^+$  signal after all selection criteria, and comparison with  $14.7\text{fb}^{-1}$  of data. The values shown for the signal assume a charged Higgs boson mass of 200 or 1000 GeV, with a cross section times branching fraction  $\sigma(pp \rightarrow [b]tH^\pm) \times \text{BR}(H^\pm \rightarrow \tau\nu)$  corresponding to  $\tan\beta = 60$  in the hMSSM benchmark scenario. The systematic and statistical uncertainties are given, respectively. Sources of systematic uncertainty are correlated amongst backgrounds when evaluating the uncertainty on the total background.

Source of systematic uncertainty	Impact on the expected limit (in %)	
	$m_{H^+} = 200\text{ GeV}$	$m_{H^+} = 1000\text{ GeV}$
Experimental		
luminosity	1.5	0.9
trigger	< 0.1	< 0.1
$\tau_{\text{had-vis}}$	1.0	1.4
jet	3.0	0.2
$E_{\text{T}}^{\text{miss}}$	< 0.1	< 0.1
Fake factors	0.8	4.7
Signal and background models		
$t\bar{t}$ modelling	13.2	3.5
$H^+$ signal modelling	1.4	1.4

# Charged Higgs $H^\pm \rightarrow tb$ search

- **BDT variables:**

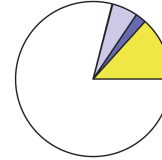
- The leading jet  $p_T$ .
- The mass of the  $bb$  pair with smallest DR.
- The  $p_T$  of the fifth jet, with the jets ordered by transverse momentum with the b-tagged jets first and then the non-b-tagged jets.
- The second Fox-Wolfram moment calculated using all jets and leptons.
- The average DR of all  $bb$  pairs.
- The DR of the lepton and the  $bb$  pair with smallest DR.
- The mass of the untagged jet pair with smallest DR.
- The scalar sum of ET calculated using all jets.
- The mass of the  $bb$  pair with largest  $p_T$ .
- The mass of the  $bb$  pair with largest mass.
- The mass of the jet triplet with largest  $p_T$ .
- The centrality, defined as the ratio of the scalar sum of the  $p_T$  of all jets and leptons over the total visible energy.

- Background Composition:

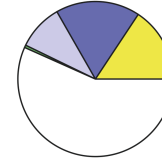
ATLAS Simulation Preliminary  
 $\sqrt{s} = 13$  TeV

$t\bar{t} + \geq 1c$ 
  $t\bar{t} + \geq 1b$   
  $t\bar{t} + \text{light}$ 
 Non- $t\bar{t}$   
  $t\bar{t} + X$

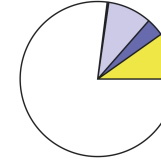
4j,2b



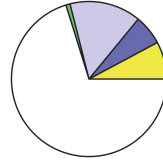
4j, $\geq 3b$



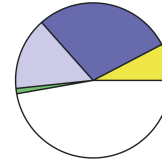
5j,2b



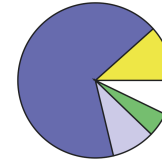
$\geq 6j, 2b$



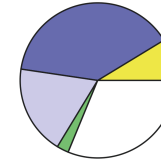
5j,3b



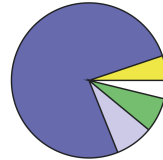
5j, $\geq 4b$



$\geq 6j, 3b$



$\geq 6j, \geq 4b$



# $H^\pm \rightarrow tb$ Systematics

Process	$4j2b$	$4j \geq 3b$	$5j2b$	$\geq 6j2b$
$t\bar{t} + \geq 1c$	10800 $\pm$ 2300	890 $\pm$ 300	10800 $\pm$ 2000	11500 $\pm$ 3600
$t\bar{t} + \geq 1b$	4580 $\pm$ 930	1650 $\pm$ 490	4440 $\pm$ 540	4800 $\pm$ 1200
$t\bar{t} + \text{light}$	160000 $\pm$ 30000	5310 $\pm$ 1550	91000 $\pm$ 17000	54000 $\pm$ 24000
Fakes	9200 $\pm$ 4400	820 $\pm$ 360	3700 $\pm$ 1600	1560 $\pm$ 670
$t\bar{t} + W$	99 $\pm$ 17	4.33 $\pm$ 0.99	130 $\pm$ 22	204 $\pm$ 40
$t\bar{t} + Z$	113 $\pm$ 21	15.7 $\pm$ 4.1	147 $\pm$ 25	270 $\pm$ 46
Single top	5900 $\pm$ 1600	243 $\pm$ 84	3470 $\pm$ 1140	2060 $\pm$ 820
Other top	4330 $\pm$ 1620	157 $\pm$ 30	1480 $\pm$ 280	630 $\pm$ 160
Diboson	420 $\pm$ 220	19 $\pm$ 12	200 $\pm$ 110	164 $\pm$ 88
$W + \text{jets}$	5250 $\pm$ 2370	183 $\pm$ 98	2300 $\pm$ 1100	1350 $\pm$ 650
$Z + \text{jets}$	1210 $\pm$ 580	42 $\pm$ 23	410 $\pm$ 210	260 $\pm$ 130
$t\bar{t}H$	63.8 $\pm$ 8.9	28.0 $\pm$ 4.9	96 $\pm$ 11	198 $\pm$ 28
$tH$	9.6 $\pm$ 2.8	5.2 $\pm$ 1.6	8.1 $\pm$ 2.4	9.9 $\pm$ 3.1
Total	202000 $\pm$ 36000	9300 $\pm$ 2000	118000 $\pm$ 23000	77000 $\pm$ 27000
Data	208329	11904	124688	84556
$H_{300}^+$	245 $\pm$ 24	124 $\pm$ 18	253 $\pm$ 20	228 $\pm$ 32
$H_{800}^+$	170 $\pm$ 16	80 $\pm$ 15	249 $\pm$ 19	477 $\pm$ 49
Process	$5j3b$	$5j \geq 4b$	$\geq 6j3b$	$\geq 6j \geq 4b$
$t\bar{t} + \geq 1c$	1170 $\pm$ 330	30 $\pm$ 11	1550 $\pm$ 530	71 $\pm$ 36
$t\bar{t} + \geq 1b$	2240 $\pm$ 460	222 $\pm$ 62	3200 $\pm$ 800	670 $\pm$ 190
$t\bar{t} + \text{light}$	3640 $\pm$ 880	24 $\pm$ 15	2600 $\pm$ 1100	34 $\pm$ 22
Fakes	260 $\pm$ 130	19.9 $\pm$ 9.3	300 $\pm$ 130	1.2 $\pm$ 0.6
$t\bar{t} + W$	8.3 $\pm$ 1.8	0.19 $\pm$ 0.07	20.8 $\pm$ 4.6	1.24 $\pm$ 0.39
$t\bar{t} + Z$	27.1 $\pm$ 5.9	4.8 $\pm$ 1.5	66 $\pm$ 12	17.9 $\pm$ 4.2
Single top	218 $\pm$ 85	8.1 $\pm$ 5.0	210 $\pm$ 100	21 $\pm$ 14
Other top	87 $\pm$ 17	6.3 $\pm$ 2.5	66 $\pm$ 16	8.3 $\pm$ 2.3
Diboson	15.6 $\pm$ 9.6	0.39 $\pm$ 0.29	14.4 $\pm$ 8.3	2.0 $\pm$ 1.3
$W + \text{jets}$	165 $\pm$ 100	2.3 $\pm$ 3.1	106 $\pm$ 54	10.4 $\pm$ 7.0
$Z + \text{jets}$	37 $\pm$ 27	0.72 $\pm$ 0.65	14.7 $\pm$ 7.9	1.17 $\pm$ 0.74
$t\bar{t}H$	49.7 $\pm$ 7.0	11.8 $\pm$ 2.3	119 $\pm$ 18	44.9 $\pm$ 9.2
$tH$	4.4 $\pm$ 1.3	1.02 $\pm$ 0.35	5.9 $\pm$ 1.9	1.92 $\pm$ 0.68
Total	7900 $\pm$ 1500	331 $\pm$ 94	8300 $\pm$ 1900	890 $\pm$ 240
Data	10755	418	11561	1285
$H_{300}^+$	173 $\pm$ 23	24.1 $\pm$ 4.0	201 $\pm$ 31	62 $\pm$ 12
$H_{800}^+$	138 $\pm$ 21	20.0 $\pm$ 4.3	366 $\pm$ 51	117 $\pm$ 24

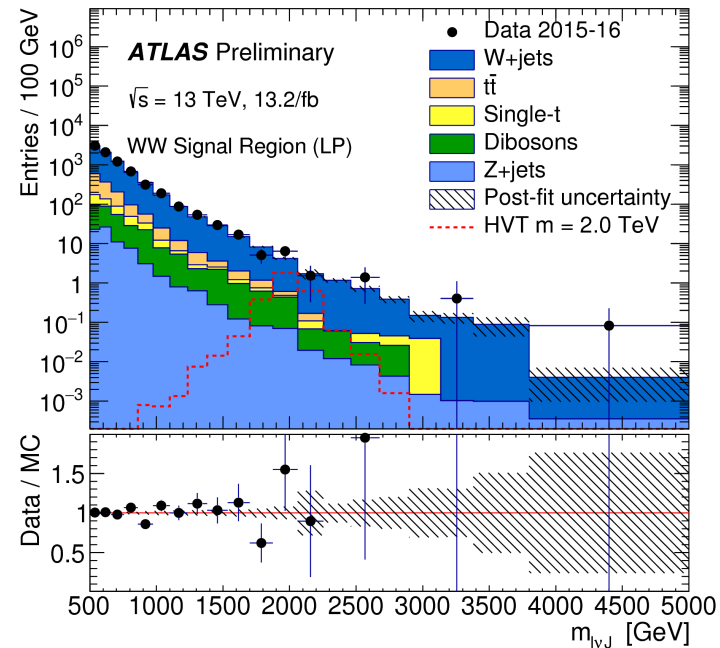
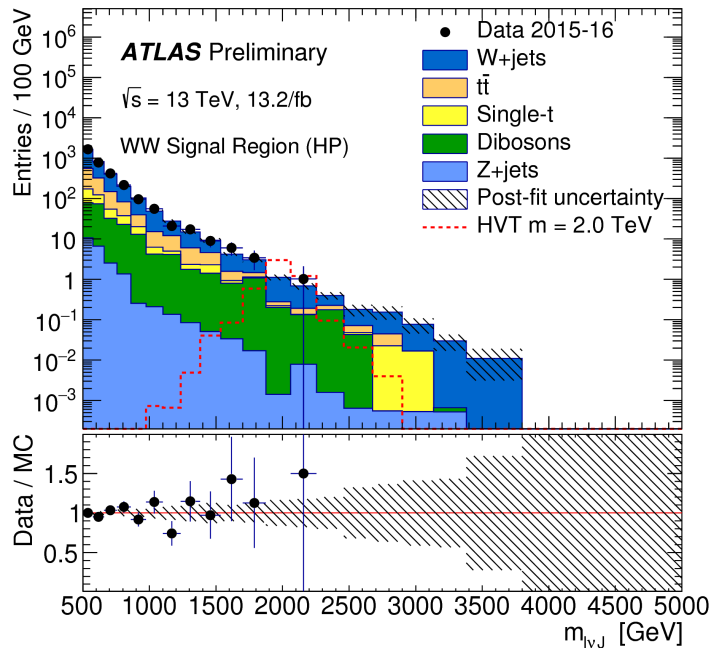
Table 1: Expected event yields of the SM background processes and observed data in all categories. The top box corresponds to the CR and the bottom one to the SR. *Single top* contribution refers to  $Wt$  production, whereas *other top* includes the  $Zt$  as well as s- and t-channel production. The quoted uncertainties include both statistical and systematical components. The prediction has not been fitted to the data. The  $H^+$  signal yields for the 300 and 800 GeV mass hypotheses and an assumed cross section of 1 pb are also shown. A value of  $13.2 \text{ fb}^{-1}$  has been assumed for the integrated luminosity.

Uncertainty Source	$\Delta\mu(H_{300}^+)$		$\Delta\mu(H_{800}^+)$	
$t\bar{t} + \geq 1b$ modelling	+0.53	-0.53	+0.07	-0.07
Jet flavour tagging	+0.30	-0.29	+0.07	-0.07
$t\bar{t} + \geq 1c$ modelling	+0.23	-0.22	+0.03	-0.03
Background model statistics	+0.19	-0.19	+0.05	-0.05
Jet energy scale and resolution	+0.18	-0.17	+0.03	-0.03
$t\bar{t} + \text{light}$ modelling	+0.16	-0.16	+0.03	-0.03
Other background modelling	+0.15	-0.14	+0.03	-0.03
Jet-vertex association, pileup modelling	+0.12	-0.11	+0.01	-0.01
Luminosity	+0.12	-0.12	+0.01	-0.01
Light lepton ( $e, \mu$ ) ID, isolation, trigger	+0.01	-0.01	< +0.01	< -0.01
Total systematic uncertainty	+0.72	-0.79	+0.13	-0.11
$t\bar{t} + \geq 1b$ normalisation	+0.36	-0.36	+0.03	-0.03
$t\bar{t} + \geq 1c$ normalisation	+0.15	-0.14	+0.02	-0.02
Total statistical uncertainty	+0.44	-0.43	+0.08	-0.08
Total	+0.84	-0.90	+0.15	-0.13

Table 3: Summary of the effects of the systematic uncertainties on  $\mu$  for an  $H^+$  signal with a mass of 300 GeV (left) and 800 GeV (right). Due to correlations between the different sources of uncertainties, the total systematic uncertainty can be different from the sum in quadrature of the individual sources. The normalisation factors for both  $t\bar{t} + \geq 1b$  and  $t\bar{t} + \geq 1c$  are included in the statistical component.

# $H \rightarrow WW \rightarrow l\nu qq$ search

Selection		SR: HP (LP)	W CR: HP (LP)	$t\bar{t}$ CR: HP (LP)
$W \rightarrow l\nu$ selection	Number of signal leptons	1		
	Number of vetoed leptons	0		
	Number of vetoed leptons	0		
	$E_T^{\text{miss}}$	$> 100 \text{ GeV}$		
	$p_T(l\nu)$	$> 200 \text{ GeV}$		
$W/Z \rightarrow J$ selection	Number of large- $R$ jets	$\geq 1$		
	Passing the $D_2^{(\beta=1)}$ cut	yes (no)	yes (no)	yes (no)
	$ m_{W/Z} - m_J $	$< 15 \text{ GeV}$	$> 15 \text{ GeV}$	$< 15 \text{ GeV}$
Topology cuts	$p_T(l\nu)/m_{WV}$	$> 0.4$		
	$p_T(J)/m_{WV}$			
Top-quark veto	Number of $b$ -tagged jets	0		$\geq 1$





# $H \rightarrow WW \rightarrow lvqq$ yields and Syst

	$WW$ signal region	$W$ +jets control region	$t\bar{t}$ control region
High-purity category			
$W$ +jets	$1810 \pm 63$	$3182 \pm 65$	$215 \pm 12$
$t\bar{t}$	$654 \pm 50$	$1020 \pm 33$	$2940 \pm 70$
Single- $t$	$163 \pm 14$	$200 \pm 15$	$322 \pm 23$
$Z$ +jets	$18.0 \pm 3.8$	$53 \pm 6$	$12 \pm 2$
Diboson	$192 \pm 31$	$70 \pm 11$	$19.0 \pm 3.8$
Total SM	$2830 \pm 80$	$4530 \pm 80$	$3500 \pm 80$
Data	$2822 \pm 53$	$4534 \pm 67$	$3509 \pm 59$
Low-purity category			
$W$ +jets	$5630 \pm 94$	$7320 \pm 110$	$706 \pm 37$
$t\bar{t}$	$730 \pm 50$	$1410 \pm 47$	$3100 \pm 89$
Single- $t$	$178 \pm 14$	$290 \pm 22$	$420 \pm 31$
$Z$ +jets	$66.6 \pm 4.8$	$134.1 \pm 7.7$	$17.7 \pm 2.8$
Dibosons	$215 \pm 34$	$150 \pm 23$	$22 \pm 4$
Total SM	$6820 \pm 80$	$9310 \pm 125$	$4260 \pm 120$
Data	$6849 \pm 83$	$9276 \pm 96$	$4270 \pm 65$

Main systematic uncertainties:

- Scale and Resolution of  $D_2^{(\beta=1)}$
- Energy and mass scale of the wide-R jets
- background estimate uncertainties, uncertainty on the shape of the  $W$ +jets background is obtained by comparing the  $m(lvJ)$  shape distribution in simulation and in data in the  $W$ +jets control region (separately for events in low and high mass sidebands)

Postfit uncertainties

# $D_2^{(\beta=1)}$

$$D_2^{(\beta)} = \frac{e_3^{(\beta)}}{(e_2^{(\beta)})^3}.$$

$$e_2^{(\beta)} = \frac{1}{p_{TJ}^2} \sum_{1 \leq i < j \leq n_J} p_{Ti} p_{Tj} R_{ij}^\beta,$$

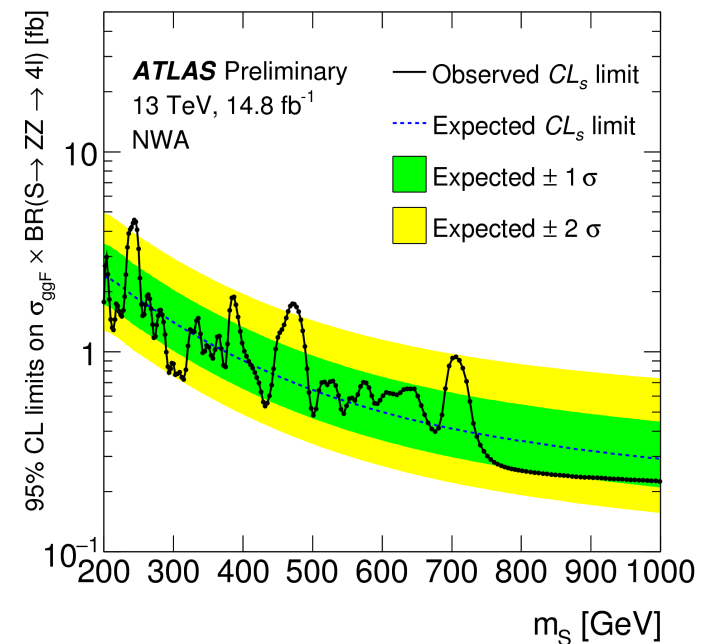
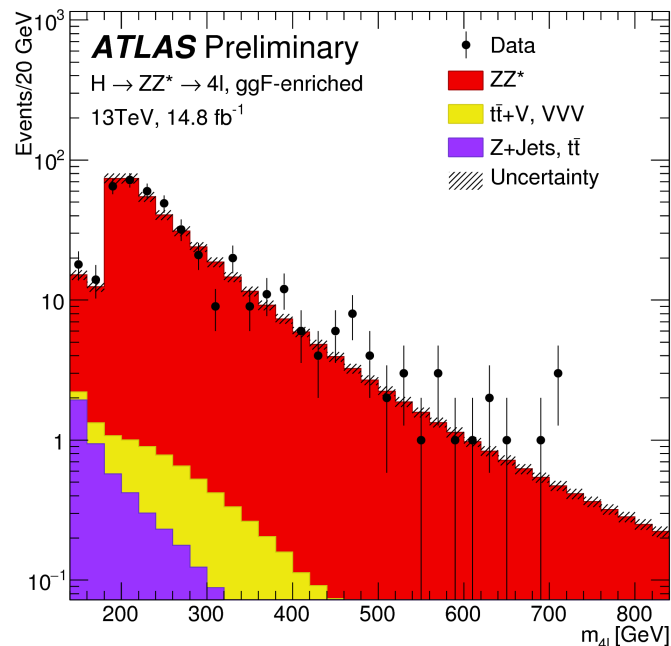
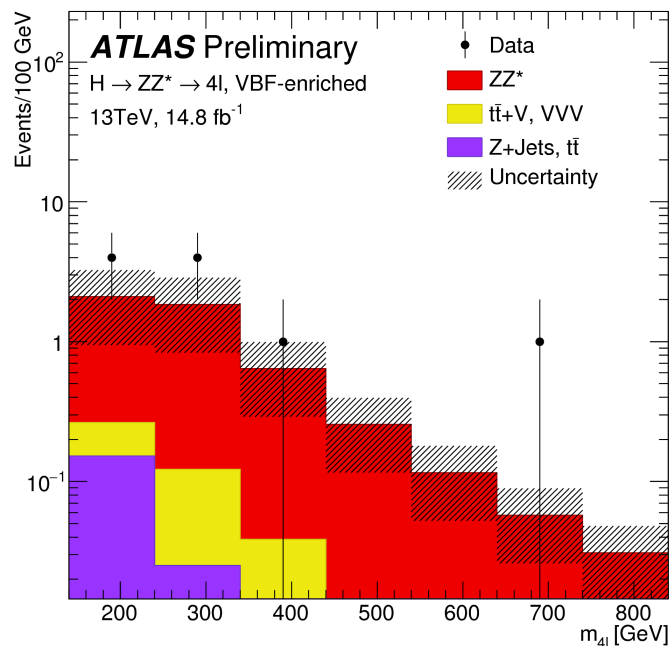
$$e_3^{(\beta)} = \frac{1}{p_{TJ}^3} \sum_{1 \leq i < j < k \leq n_J} p_{Ti} p_{Tj} p_{Tk} R_{ij}^\beta R_{ik}^\beta R_{jk}^\beta,$$

Substructure variable used to discriminate boosted W/Z decays to quarks from QCD (non top-quark) jets, based on power-counting.

Purpose is to separate 2-prong decays from 1-prong ones.

# $H \rightarrow ZZ \rightarrow 4l$ search

- **ATLAS-CONF-2016-079,  $14.8 \text{ fb}^{-1}$  @ 13 TeV**
- Same selection as SM  $H \rightarrow ZZ \rightarrow 4l$  ( $l=e,\mu$ ), but requires both Z on-shell
- VBF-enriched category:  $m_{jj} > 400 \text{ GeV}$  and  $\Delta\eta_{jj} > 3.3$
- ggH-enriched category: the rest
- Limits set for VBF and ggH production and 4.07 MeV, 1%, 5% and 10% widths



# $H \rightarrow ZZ \rightarrow 4l$ search (2)

## • Main Systematics:

- $ZZ^*$  background uncertainty
- uncertainty on subdominant gluon initiated ZZ production ( $gg \rightarrow (H^*) \rightarrow ZZ$ ) is also taken into account.

Final state	$ZZ^*$	$Z + \text{jets}, t\bar{t}, WZ$	$t\bar{t}V, VVV$	Expected	Observed
$4\mu$ ggF-enriched	$125 \pm 10$	$0.95 \pm 0.14$	$1.57 \pm 0.09$	$127 \pm 10$	128
$2e2\mu$ ggF-enriched	$205 \pm 17$	$2.5 \pm 0.4$	$2.75 \pm 0.17$	$211 \pm 17$	199
$4e$ ggF-enriched	$83 \pm 7$	$1.47 \pm 0.22$	$1.28 \pm 0.08$	$86 \pm 7$	111
VBF-enriched	$4.6 \pm 2.8$	$0.18 \pm 0.05$	$0.268 \pm 0.016$	$5.1 \pm 2.8$	10
Total	$418 \pm 35$	$5.1 \pm 0.7$	$5.87 \pm 0.35$	$429 \pm 35$	448

Full uncertainties are provided.

# $H \rightarrow ZZ \rightarrow llqq$ and $\nu\nu qq$ Searches

## $H \rightarrow ZZ \rightarrow llqq$

Process	Merged analysis		Resolved analysis	
	high purity	low purity	tagged	untagged
	Signal regions			
$Z$ +jets	$576 \pm 22$	$1230 \pm 33$	$409 \pm 18$	$19900 \pm 140$
Diboson	$49 \pm 7$	$51 \pm 5$	$54 \pm 6$	$670 \pm 40$
Top quark	$4 \pm 1$	$5.9 \pm 1.0$	$131 \pm 6$	$291 \pm 28$
Total background	$629 \pm 22$	$1287 \pm 34$	$594 \pm 18$	$20861 \pm 140$
Data	606	1270	608	20857
$H$ (400 GeV)	$1.6 \pm 0.2$	$4.3 \pm 0.7$	$107 \pm 6$	$626 \pm 21$
$H$ (700 GeV)	$168 \pm 4$	$88.2 \pm 2.9$	$20.0 \pm 1.2$	$71.4 \pm 3.3$
$H$ (1600 GeV)	$35.9 \pm 0.8$	$24.0 \pm 0.6$	$1.00 \pm 0.09$	$1.60 \pm 0.08$

## $H \rightarrow ZZ \rightarrow \nu\nu qq$

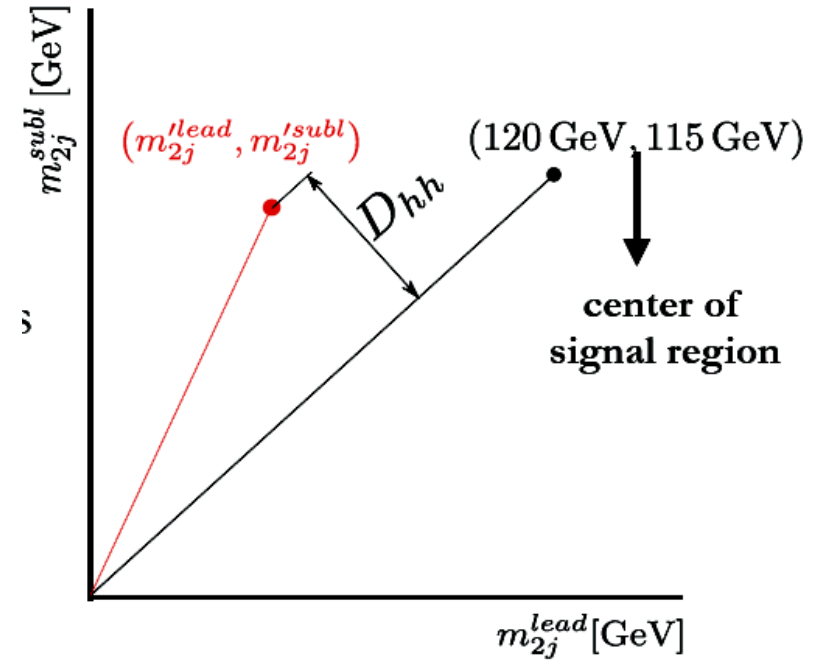
Process	Merged analysis	
	high-purity	low-purity
$Z$ +jets	$1251 \pm 56$	$3130 \pm 79$
$W$ +jets	$881 \pm 45$	$2092 \pm 75$
Diboson	$202 \pm 14$	$227 \pm 10$
$t\bar{t}$ + single top	$557 \pm 85$	$610 \pm 100$
Total background	$2891 \pm 50$	$6059 \pm 76$
Data	2859	6044
$H$ (1600 GeV)	$63.7 \pm 1.9$	$46.2 \pm 1.4$

The dominant uncertainties are the  $D_2^{\beta=1}$  and mass scale uncertainty, which are of the order of 10%

# $hh \rightarrow bbbb$ Regions

## Resolved Analysis:

- Pairing chosen to minimize the distance  $D_{hh}$
- Center of the signal region is: (120 GeV, 115 GeV) - account for energy losses through semi-leptonic decays
- The center corresponds to the median values of the narrowest intervals that contain 90% of the signal in simulation

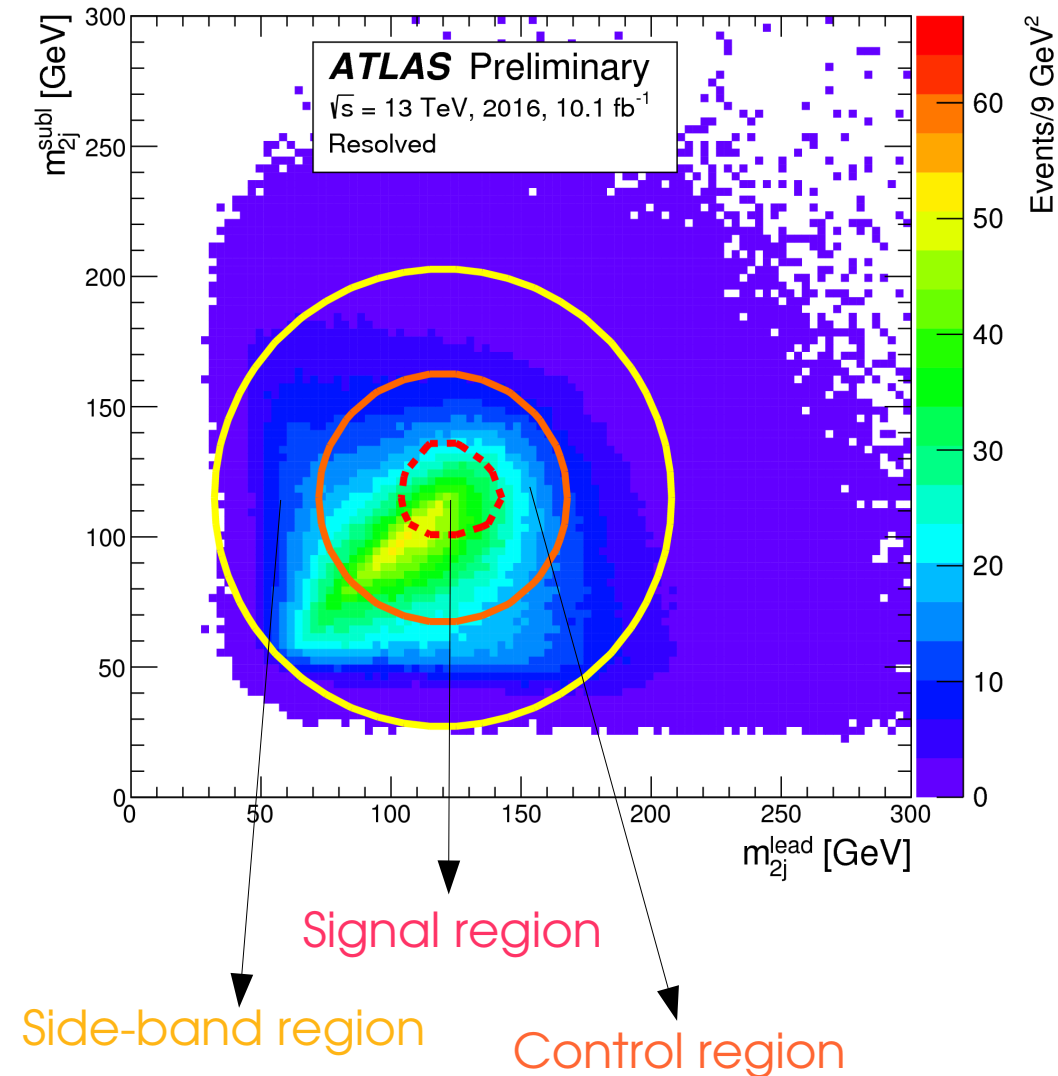


$$D_{hh} = \sqrt{(m_{2j}^{lead})^2 + (m_{2j}^{subl})^2} \left| \sin \left( \tan^{-1} \left( \frac{m_{2j}^{subl}}{m_{2j}^{lead}} \right) - \tan^{-1} \left( \frac{115}{120} \right) \right) \right|$$

# $hh \rightarrow bbbb$ Regions

## Resolved Analysis:

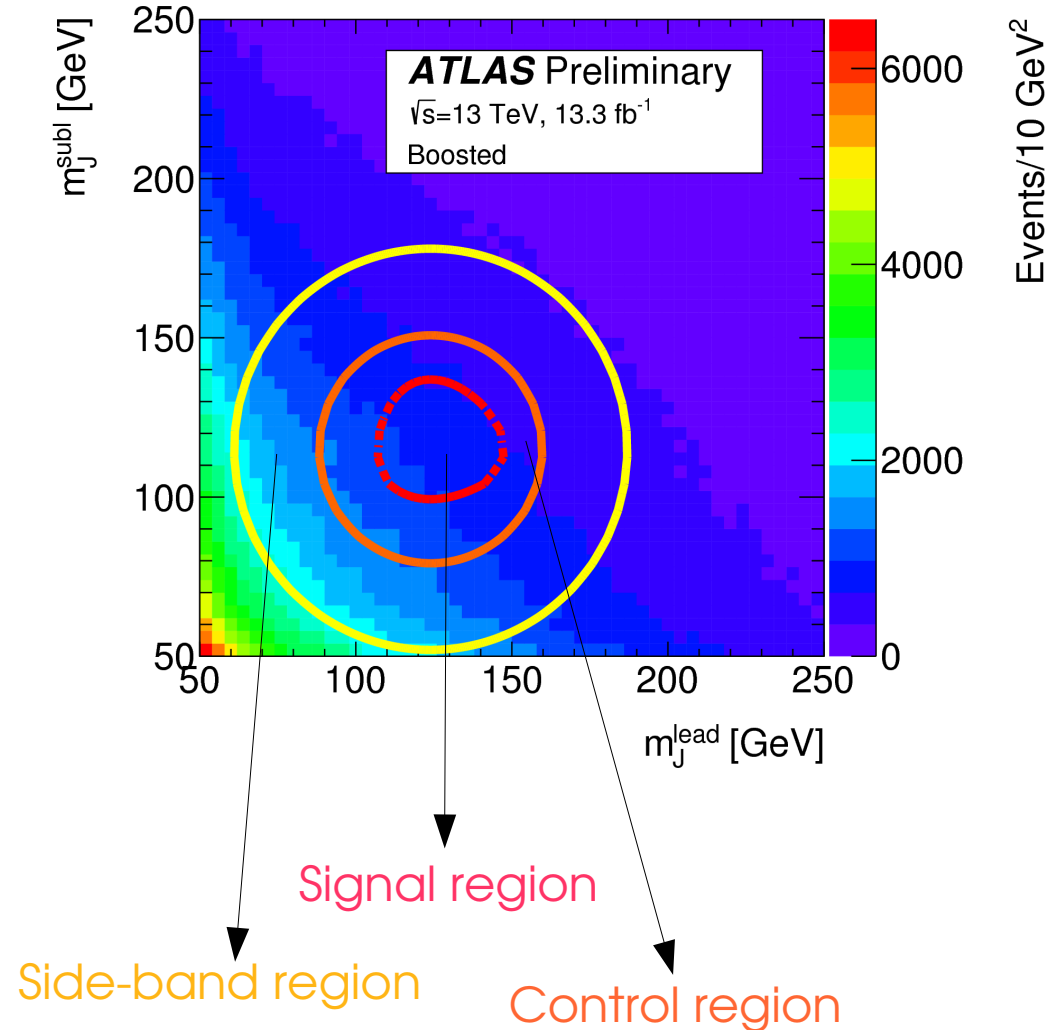
- Side-Band Region:
  - Used to extrapolate to 4-tag SR by using 2-tag events
- Control Region:
  - Verify the QCD modelling
  - Assess systematics
- Signal Region:
  - Statistical analysis



# $hh \rightarrow bbbb$ Regions

## Boosted Analysis:

- Side-Band Region:
  - Derive the normalisation of the multijet and  $t\bar{t}$  backgrounds
- Control Region:
  - Verify the background models
  - Assign systematic uncertainties
- Signal Region:
  - Statistical analysis





# $hh \rightarrow bbbb$ Yields and Systematics

## Resolved Analysis

## Boosted Analysis

Sample	2015 Signal Region	2016 Signal Region
Multijet	$1\,131 \pm 68$	$3\,670 \pm 200$
$t\bar{t}$	$57 \pm 34$	$190 \pm 110$
Total	$1\,189 \pm 76$	$3\,860 \pm 230$
Data	1 231	3 990
SM $hh$	$0.47 \pm 0.12$	$1.5 \pm 0.4$
$G_{\text{KK}}^*$ (800 GeV), $k/\bar{M}_{\text{Pl}} = 1$	$8 \pm 3$	$24 \pm 8$

Sample	2-tag-split	3-tag	4-tag
Multijet	$2\,310 \pm 240$	$515 \pm 41$	$32.6 \pm 7.6$
$t\bar{t}$	$460 \pm 170$	$81 \pm 37$	$5.7 \pm 5.2$
Total	$2\,770 \pm 130$	$596 \pm 39$	$38.3 \pm 9.0$
Data	2 813	671	32
$G_{\text{KK}}^*$ (2 TeV), $k/\bar{M}_{\text{Pl}} = 1$	$0.17 \pm 0.10$	$0.31 \pm 0.06$	$0.15 \pm 0.06$

Source	2015			2016		
	Background	SM $hh$	$G_{\text{KK}}^*$ (800 GeV)	Background	SM $hh$	$G_{\text{KK}}^*$ (800 GeV)
Luminosity	-	2.1	2.1	-	3.7	3.7
JER	-	5.7	3.3	-	5.4	3.5
JES	-	6.4	1.3	-	6.6	1.3
$b$ -tagging	-	23	35	-	23	35
Theoretical	-	9.7	4.2	-	9.7	4.2
Multijet	5	-	-	5	-	-
$t\bar{t}$	58	-	-	58	-	-
Total	5.5	26	35	5.5	27	36

Source	2-tag-split		3-tag		4-tag	
	Background	$G_{\text{KK}}^*$ (2 TeV)	Background	$G_{\text{KK}}^*$ (2 TeV)	Background	$G_{\text{KK}}^*$ (2 TeV)
Luminosity	-	2.9	-	2.9	-	2.9
JER	-	0.1	-	0.1	-	0.3
JMR	-	12	-	12	-	12
JES/JMS	-	4.5	-	4.2	-	3.3
$b$ -tagging	-	58	-	15	-	38
Theoretical	-	2.7	-	2.3	-	2.4
Bkg Estimate	4.4	-	4.6	-	21	-
Statistical	0.5	1.4	1.1	1.0	1.2	1.3
$t\bar{t}$	1.6	-	4.7	-	10	-
Total Sys	4.7	59	6.6	20	24	40

# $hh \rightarrow WW\gamma\gamma$ and $bb\gamma\gamma$ Searches

- $hh \rightarrow WW\gamma\gamma$ ,  $13.3 \text{ fb}^{-1}$  :**

- Final state  $\gamma\gamma lvqq'$
- $2\gamma$ , 2 non  $b$ -tagged jets
- $105 \text{ GeV} < m_{\gamma\gamma} < 160 \text{ GeV}$

- Results** (assuming SM Higgs BR):

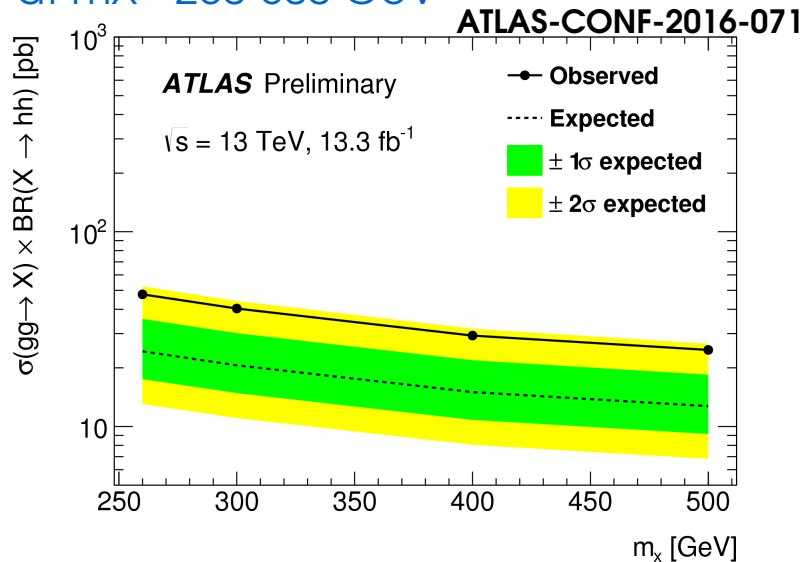
- Non-resonant search:

$$\sigma(pp \rightarrow hh) < 25.0 \text{ pb}$$

- Resonant search, limits on  $\sigma(pp \rightarrow X \rightarrow hh)$ :

$47.7\text{-}24.7 \text{ pb}$  (expected  $24.3\text{-}12.7 \text{ pb}$ )

at  $m_X = 260\text{-}500 \text{ GeV}$



- $hh \rightarrow bb\gamma\gamma$ ,  $3.2 \text{ fb}^{-1}$  :**

- $2\gamma$ , 2  $b$ -tagged jets
- $95 \text{ GeV} < m_{bb} < 135 \text{ GeV}$
- $105 \text{ GeV} < m_{\gamma\gamma} < 160 \text{ GeV}$

- Results** (assuming SM Higgs BR):

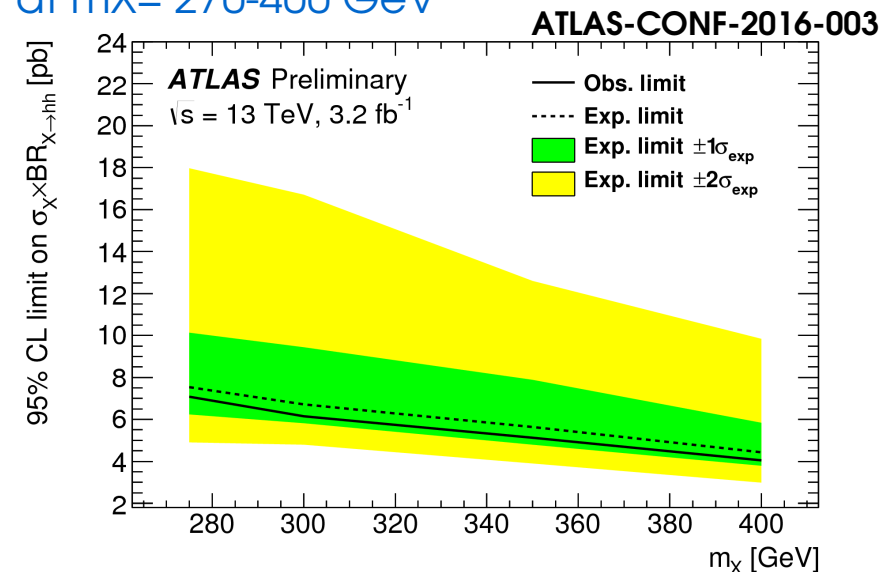
- Non-resonant search:

$$\sigma(pp \rightarrow hh) < 3.9 \text{ pb}$$

- Resonant search, limits on  $\sigma(pp \rightarrow X \rightarrow hh)$ :

$7.0\text{-}4.3 \text{ pb}$  (expected  $7.8\text{-}4.5 \text{ pb}$ )

at  $m_X = 270\text{-}400 \text{ GeV}$



Fermion family	Type-I	Type-II	Lepton-specific	Flipped	Type-III
u	$\Phi_2$	$\Phi_2$	$\Phi_2$	$\Phi_1$	$\Phi_1, \Phi_2$
d	$\Phi_2$	$\Phi_1$	$\Phi_2$	$\Phi_1$	$\Phi_1, \Phi_2$
e	$\Phi_2$	$\Phi_2$	$\Phi_1$	$\Phi_2$	$\Phi_1, \Phi_2$